Master's Degree programme
in Environmental Sciences

Università
Ca'Foscari
Venezia

Final Thesis

Extreme value analysis of precipitation in Pakistan

Supervisor
Ch. Prof. Carlo Gaetan

Graduand
Muhammad Attiq Khan
Matricolation number
877302

Ca' Foscari
Dorsoduro 3246
30123 Venezia

Academic Year
2020/2021

Abstract

The climate of the earth has been changing with time, over millions of years and mostly in the previous two centuries with the involvement of greenhouse effect, which has put the climate at stake in an unprecedented level. Extreme values in precipitation are amongst the most critical and famous subject in the field of climate sciences. To analyse our data, we have used the extreme value analysis for our results, since our data contains annual maximum value of precipitation, therefore we have adopted the block maxima approach to check the positive/negative trends, maximum values. To check the results, the model adopted is Generalized Extreme Value (GEV) estimated with the Maximum Likelihood Estimation (MLE) method.

The results of our analysis have been obtained from our data of precipitation recorded at 28 different stations in Pakistan from the year 1985 to 2016. From the model results, Gilgit station, which is at the north of Pakistan, has the least maximum value of precipitation, i.e. 64.5 same as Panjgur in the period shows the best model fit results amongst all the station. The stations that represent worst model fits are: Sialkot, Jhelum, Lahore, Khanpur, Badin, Jiwani, Chhor, Jacobabad and Karachi, compared to the other stations that show better model fit.

The stations with high variations do not give us the better model fit results. The quantiles plot shows that, for high values the model fit is uncertain for almost all the stations, and the residuals are drifting at higher upper-end tail distribution; apart from that almost all the quantile plots show us the normal distribution with better model fits. The return level for the maximum extreme lies between 20 to 50 years except for few stations which include Zhob, Khuzdar and other.

Contents

1 Introduction

The climate of the earth has been changing with time, over millions of years and mostly in the previous two centuries with the involvement of the greenhouse effect, which has put the climate at stake at an unprecedented level. Change of solar cycle patterns, atmospheric changes, impacts of El-Nino southern oscillation (ENSO), sea ice extent changes, natural biosphere variability are the reasons that show the evidence of both external and internal references to change and variability. The different earth components are also subjected to show variations in response to all these variabilities. The surface air temperature has increased around 2.9°C in Boreal Asia over the last century. The nations located in Asia subjected to the greenhouse and climate change effects are expected to have more shift patterns of floods, storms, droughts, and the increase in sea level rise. The historical evidences of these regions show that they are more vulnerable to the variation in monsoons, tropical cyclones and El-Nino southern oscillation (Farooqi et al., 2005).

Extreme values in precipitation are amongst the most critical and famous subjects in the field of climate sciences. Its intensity and variability of extreme values are evident in climate change. Many studies in these aspects and its findings have proved that it varies significantly according to the location and period. It also impact human lives, community, welfare and society, agricultural activities and economies (Smadi and Zghoul, 2006), (Fowler et al., 2008), (Nikhil Raj and Azeez, 2012). It has become a priority of the researchers to understand the variation of extreme values in precipitation over long term temporal scales, and many researchers have evaluated the variation in extremes of precipitation in different regions of the world (Brunetti et al., 2001), (Łupikasza et al., 2011), (Park, 2011), (Burauskaite-Harju et al., 2012), (Iwasaki, 2012), (Gillies et al., 2012), (Li et al., 2012) and various studies has shown the trends in increasing heavy precipitation (Nastos and Zerefos, 2008), (Burt and Ferranti, 2012), (Iwasaki, 2012), (Deshpande et al., 2012).

Regional analysis in extreme precipitation indicates non-uniform and complex spatial patterns (Aleem-ul Hassan et al., 2010), (Raziei et al., 2012). Many researchers have found the significant trends of extremes in precipitation in different regions around the world (Dravitzki and McGregor, 2011), (Naumann et al., 2012). Similarly, numerous studies of seasonal variability in extreme precipitation have also illustrated decreasing trend (Schmidli and Frei, 2005), (Zolina et al., 2008), (Lupikasza, 2010). Although, extremes of precipitation and its impacts have created significant interest in the community of scientists. Many scientist have explained that heavy precipitation is the major reason to cause severe floods all over the world (Frei and Schär, 2001), (Svensson and Jakob, 2002), (Kunkel, 2003), (Park, 2011), which is also obvious in Pakistan, where there are many damages caused in the recent years (Afzal and ul Zaman, 2010), (Aleem-ul Hassan et al., 2010), (Aziz and Tanaka, 2011).

Recently, with an increase in the concern over the climate change impacts, scientists have implemented various statistical tools and techniques to highlight the concerning trends within the time and space of precipitation and its extreme events (Hussain and Lee, 2013). The non-parametric approach has been implemented mostly to assure the results of previous techniques, which includes shifting averages and regression (Hussain and Lee, 2013). In this context, most of the studies in a variation on the precipitation have been done recently, which

provided a great knowledge into the significancy and the direction of the precipitation trends in certain regions (Smadi and Zghoul, 2006), (Samba and Nganga, 2012).
Changes in the extreme precipitation patterns and their impacts on water resources are one of the main climatic concerns these days. The prediction of these changes is ultimately significant for regions which are already facing some concerns and are under stress, for instance: the regions where there is water shortage because of the dry climatic properties and where the season precipitation is very high regardless of its dry conditions (Hussain and Lee, 2013). The trends of precipitation extreme are highly dependent on the period of study and seasonality; therefore, a specific approach that could evaluate the high variability in precipitation over space and time is required. However, the results of the trends are strongly dependent on the values at the beginning and at the end of the time series (Lupikasza, 2010). An overlook of the trends in indices of precipitation extremes moving trends for a period of 30 years was observed to identify the changes in the trends to analyse significant extreme precipitation. (Hussain and Lee, 2013).

1.1 Country Profile

Pakistan has a long extent of latitude extending from Himalayan mountains situated in the north and the Arabian Sea in the south, located in the subtropic and temperate region. It has a population of about 216.6 million people, which are mostly at stake and vulnerable because of climate change. A large portion of the people in Pakistan live in river deltas or low coastal areas, where flooding and sea-level rise are one of the devastating impacts of the increase in global temperature and climate change. Many regions of Pakistan, climatically, are from semi-arid to arid, where temporal and spatial variability is significantly variable in climate parameters. Annual rainfall is mostly in the monsoon season, which consists of 59 %, and it plays an important part in the recharging of the Himalayan region. In winter, in the regions beyond 35°N, the precipitation is in the form of ice and snow, which let the rivers to flow throughout the year (Farooqi et al., 2005). The north consists of the mountains where the climate is from humid to arid, and the south along the coast is limited to a narrow strip. Between north and south, the climate is mostly tropical and continental (Farooqi et al., 2005).
Pakistan's geography extends over 796,095 KM^2 areas with a huge diversity in precipitation and temperature. In the southern half, eastern areas receive precipitation mainly from the western part of the region in the monsoon season from June to September, whereas the western and the northern areas mainly receive precipitation from the western disturbance in weather from December to March. In summer, monsoon precipitation is accounted for 60% of total precipitation. Annually, 3/4 of the country receives less than 250 millimetres of rainfall except in the southern Himalayan slopes and sub mountainous region in the north, where it receives annual rainfall over 760 to 2000 mm. The northern region is very high above sea level with some gigantic peaks like K2 (8611 meters), and also the region is rich in glacial resources consisting of one of the worlds largest glaciers such as Siachen, which is 70 km long and Biafo which is 63 km long, which helps in feeding the Indus river and connected tributaries (on Dams, 2000). The temperature in the northern regions goes lower as –50°C

during winter and remains around 15°C during summer. The southern and western regions of Pakistan are consisted of the Indus river plains and plateaus of Balochistan. The boundaries around the Indus river is extended to 520,000 km^2 and cover 65% of the total area which flows through all the provinces of Pakistan. Pakistan has one of the most extensive contiguous irrigation systems, mainly dependent on the Indus River basin, which covers 95% of the irrigation system (Chaudhry, 2017).
Indus plain receives 230 mm of average rainfall, the temperature variation between the lower and upper basin plains is quite dominant, where mean temperature in winter is from 14 to 20 °C in the lower plain, while in the upper plain regions, its from 2 to 23 °C. The summer average temperature is 42 to 44 °C in the lower plain and 23 to 49 °C in the upper plains. Baluchistan is the wildest province of the country and has variant mountain ranges with an altitude of 600 meters on average, and most of the parts are consisted of deserts with the least water resources and rivers flowing through the region. The country also contains deserts in Sindh and Punjab, namely Thar and Cholistan, where rainfall is less than 210 mm over the year (Chaudhry, 2017).
Pakistan's economy is totally dependent on agriculture, and IPCC's fifth assessment report highlights the climate change impacts and its severity. The threats are evident due to its significant geographic placement, demographic trends, least adaptive capacity, also including the socio-economic factors (Hijioka et al., 2014). The projections of the climate change described in the AR5 report for South Asia represents that the global temperature rise will be higher than the mean global temperature increase, which will impact the glaciers loss at a high rate and affect the regional climate and also the precipitation patterns. The monsoon cycle will also be affected due to certain changes which will affect the timescale of rainfall and its capacity, efficiency and the productivity of agriculture (Chaudhry, 2017).

1.2 Pakistan Meteorology Department

The Pakistan Meteorological Department (PMD) is the prime authority responsible for monitoring climate activities and weather forecasting in the country. It provides meteorological services across Pakistan to various users. In addition to routine meteorological services such as daily weather recording, processing, storage and forecasting and distribution, the department is also responsible for the areas connected with meteorology such as; agriculture, hydrology, flood forecasting, astronomy and astrophysics, seismology, geomagnetism, ozone monitoring, weather change, drought monitoring etc. All kinds of meteorology related disasters, i.e. storms, cyclones, torrential rains, tornadoes, etc., hydro-meteorological related disasters such as floods, droughts etc. In geophysics, earthquakes, ozone depletion, ionospheric disturbances, etc., are also monitored. The normal climate conditions of Pakistan for the period of 30-years, i.e., 1931-60, 1961-90 and 1971-2000, can be easily accessed and are also available and published in the department. The department also has the monthly data of all-weather stations in digitized form. However, daily and hourly daily data have not yet been digitized but can be obtained from its archives (Sheikh et al., 2009).

2 Literature Review

From the period of 1951 to 2000, 10 to 15 % of the summer and winter rainfall was observed to be decreased in coastal and arid plain areas while 18 to 32 % was observed to be increased in the summer monsoon season, and relative humidity was decreased by 5 % in Balochistan (Chaudhry, 2017). However, 17 to 64 percent of the decrease in rainfall was observed over the last 100 years events during the El-Nino strong events. Storms, cyclones and depressions in the Arabian sea and bay of Bengal have been increased in the last years of the 20^{th} century, which has affected some countries, including Pakistan (Farooqi et al., 2005). In the 20^{th} century and 7 years of 21^{st} century which includes the data from 18 stations and 5 stations from the year 1914 onwards, represents the long term precipitation, where 10 years moving average in the time series analysis proved that rainfall has been decreased until 400 millimetres from 600 millimetres up to the year 1940 and an increase of 133 millimetres was observed after that period. Overall, 61 mm of the annual precipitation increase was observed at the national level, 22.6 millimetres of monsoon rainfall was increased, and 20.8 millimetres of the winter precipitation was increased (Chaudhry, 2017).
The annual mean precipitation has been significantly increasing apart from coastal areas also, the monsoon rainfall represents a similar trend. However, the winter precipitation represents the complex pattern with the decrease in the trend in highlands of West in Kirthar Ranges in Sindh and Suleman ranges in Baluchistan. In the Himalayas, it shows an increase in the precipitation trend during the period of monsoon from June to September, and precipitation slightly decreases in the winter period from December to March (Chaudhry, 2017). According to Iqbal et al. (2014), the yearly precipitation and temperature for the future trends for 2050 and 2080 under different emission scenarios, the temperature increase in 2080 by using the GCM model will increase by 4.38°C in Pakistan, and this increase will be higher in northern areas in winter and summer. Also, the temperature increase will be higher comparatively in winter in both south and north. The precipitation did not show any significant changes, but there is a slight increase in summer precipitation while it decreases in the winter.
The other significant studies under Pakistan meteorological department, which computed precipitation and temperature change for Pakistan in the years from 2011 to 2050 through different climate models, show that: the temperature increase is to be expected in northern areas, southern and northern Punjab, and some low regions of Khyber Pakhtunkhwa (KPK). Mixed patterns were observed for precipitation in the various regions (Chaudhry et al., 2009), and the uniform variation in the distribution of rainfall was predicted in a study conducted over the whole regions of Indus Basin (Rajbhandari et al., 2015). At the sub-level regions of the upper and lower Indus basin, the models indicated an increase in the trend of rainfall at an upper level and a decreasing trend in the lower level and slight changes were seen on the border zone. The study also predicts the increase in the number of days for rainfall and also the intensity of rainfall over the border zone (Rajbhandari et al., 2015).
In May 2015, PMD presented daily gridded down-scaled temperature and precipitation from 2010 to 2099 in time series for 4 different GCM models of climate change scenarios which shows the 3 to 5 degrees of temperature rise under 4.5 emission scenario. The rainfall has high variation according to the time and

intensity, and some peaks represent the risk of extreme events while there are also some extreme events for low precipitation indicating droughts (Chaudhry, 2017). Another model presents that by 2050, rainfall in summers will be shifted to August and that of winter to March. This trend will be continued till the end of this century. The representative concentration pathway (RCP) 4.5 indicate the increase of mm/day in mean yearly precipitation along with maxima shift to the northeast part of Pakistan by mid-century. After the mid-century, the pattern shifts of precipitation are towards the northeast part of the country. Similar behaviour is observed under RCP 8.5 scenario with lower magnitude, i.e. 2 mm/day with an increase in temporal scale (Chaudhry, 2017).

Over 70 to 50 % of the precipitation in Pakistan is linked with the monsoon in summer, while in winter, most of the precipitation is caused by the western disturbance (Hussain and Lee, 2009). Pakistan climate is characterised by irregular patterns of precipitation that is highly variable with respect to space, time, intensity, and duration, which has not been discussed much (Hussain and Lee, 2013). The period in which mostly, the precipitation, i.e. 56% in a year, falls from June to September, from which 41.3% occurs in July and August combined. Lower values are observed in winters from November to December, and from January to April, the rainfall is mainly uniform (Hussain and Lee, 2009). In the research carried by Hussain and Lee (2009), in which he has classified six regions of Pakistan according to the precipitation and weighted by a number of weather stations, where region 1 receive the least precipitation, which is 45.6% in summer and autumn is mainly dry. Region 2 receives high precipitation during the spring season, while region 3 receives most of the precipitation in winter, where summer precipitation is comparatively low. Region 4 is classified according to the high precipitation that occurs in winter and spring. Region 5 is mostly wet, which receives high precipitation in summer and also in all other seasons, which is less than summer and comparatively region 6 receives more amount of precipitation in summer only (Hussain and Lee, 2009).

Annual trends of different indices for a long term of extreme precipitation highlighted over most of Pakistan from the period of 1950 to 2010, in which positive values were prominent in spatial perspective (Hussain and Lee, 2013). The values differ with the index used however, the increase in days are significant with respect to the extreme precipitation. Initial 30 years from 1950 highlighted the increase in the trend while other 30 years from 1971 and 1981 presented downward trends (Hussain and Lee, 2013). However, in the extent of territories, both trends of positive and negative are varied and showed both upward and downward directions. The Kendall tau based results showed some variations with an increase in the number of days for heavy precipitation and its totals, however, the slope pattern with the results are similar to linear trend (Hussain and Lee, 2013). The results of daily precipitation and its extremes from the 15 weather stations across the country were analysed, which presents the spatial variability in 61 years (Hussain and Lee, 2013). However, the analysis for long-term changes is complex in precipitation extremes due to the lack of availability of long-term data. The variability in extreme precipitation has significant consequences, such as the risk of flooding, river flow, and direction that could affect engineering structures such as dams, bridges and urban drains (Hussain and Lee, 2013).

Annual mean precipitation dominates to follow the variation in a distinct latitudinal way from the south to the north. In the humid northern region, the

mean annual precipitation is less than 30 to less than 150 millimetres. This region is situated at the border of the Himalayan region and is supposed to be the core monsoon region. This region is also evident to receive a certain amount of precipitation from the westerlies system, which presents the seasonal trends. However, the higher northern parts, where a local hydro-logical cycle is extremely dependent on westerlies, presented about 0.1 to 30-millimetre decrease in the precipitation because of its geographical location (Waqas and Athar, 2019). Identically, the southern parts having arid and semi-arid climatic conditions are characterised by minimal precipitation. The southern regions have a tropical and coastal climate which has a low or minimum influence of westerlies system and monsoon (Ullah et al., 2019). The precipitation can be divided into two modes, i.e. summer and winter. Winter precipitation which is also known as pre-monsoon precipitation, is mainly because of the westerlies climate, and summer is mainly due to the monsoon. All these modes support the hydro-logical cycle across the country and the perennial flow of the Indus river basin. These two modes are the main sources of local water supply throughout the country. The variability in latitudinal trends has the benefit of creating most of the precipitation inside the country, and the increase and decrease of these two modes of precipitation can adversely affect the region (Ullah et al., 2018), (Abbas et al., 2018).

Rainy days have been increased by 0.40 days in a long-term period from 1980-2016, and the increase is more prominent in the north and eastern parts. However, the arid lands of the south and humid regions of the centre show a decrease of 0.39 days (Bhatti et al., 2020). However, the heavy precipitation days has been decreased by 0.25 for a 10 mm magnitude in north, humid and semi-arid regions of Pakistan. 0.2 days of increase was found in the east and central regions and vice versa in the south and southwest. The heavy precipitation of 20 mm follows an asymmetric pattern where it has been decreased/increased in the north-south and central parts with a rate of 0.2 days. Severe precipitation with a magnitude of 50 mm apart from a few humid region's stations, the country overall showed a declined trend. The annual total precipitation can be concluded to have an increasing trend at 0.1mm in the east and the north of the country (Bhatti et al., 2020). Only some of the stations in the core monsoon semi-arid and humid region presented a decrease of 9.9 mm during the 1980-2016 period. The mean precipitation has been increased by 0.14 mm in the monsoon regions, and the decrease of 0.1 has been observed in southern arid and northern regions (Bhatti et al., 2020). The regions with high altitude and humidity in the north exhibited a decrease in precipitation by 0.17 mm with 95^{th} percentile, and the increase of about 0.015 mm has been observed in the east and south-eastern parts. The 99^{th} percentile showed to be decreased by 0.08 mm in the coastal regions of the southwest, and the north and an increase of 0.06mm was observed in the west and central parts of the country (Bhatti et al., 2020). The indices show an increase in the trends of monsoon precipitation, and it is also suggested that it could increase its time span along with the westerlies, which has also presented some evidence of an increase in the precipitation (Zhan et al., 2017), (Bhatti et al., 2020). The Sequential Mann-Kendall test statistics based on the period of 1980 to 2016 over the regions of Pakistan referred for precipitation indices resulted that rainy days were decreased in the early 1980 period, and later increased in early 1990 years and again decreased in the early

2000 and from 2011 showed a slight increase. The heavy precipitation for total annual precipitation observed to follow the same pattern of increase/decrease in 1980/1990 (Bhatti et al., 2020).
The trend appears to increase steadily after 2005, suggesting higher frequencies of extreme cases in precipitation events in Pakistan. The magnitudinal increase or decrease of extreme precipitation is in agreement with the wet or dry events perceived in the regions of interest in the respective study (Ullah et al., 2018), where it has been possibly influenced by a large-scale abnormality in the circulation of ocean indices and require more exploration (Xie et al., 2013).
The increase of the events in the latter part of the respective study also indicates that the climatic footprints variability generated by the change in the water-cycle is evident at the regional level and therefore may increase floods observed in recent time (Gadiwala and Burke, 2019). The mean precipitation on rainy days showed little variability until 2000, and a significant gradual decrease was observed in early 2000, and a significant increasing trend was followed in the rest of the period. The 95^{th} percentile of precipitation showed a downward trend that was significant during the last ten years around 2012 and was the same afterwards. The precipitation events at the 99^{th} percentile showed to be varying in a small range for the duration of the study. However, a more pronounced decline can be observed at the end of the duration of the study, which suggests a decrease in extreme precipitation events. In general, it can be summarized that the precipitation indices have shown strong growth in trend, especially in recent years. The inflection points indicated that some changes (increase/decrease) in the P indices occurred during the study period. Extreme precipitation events of (95_{th}) percentile seemed to have decreased in recent years, while severe events (99^{th}) percentile decreased slightly in recent years (Bhatti et al., 2020). Study results for precipitation based on size and frequency are consistent with those within the context of the world's climate change. The last two indices indicate that the decreased lag is due to the regional-based average, and therefore some regions have experienced an upward/downward trend. However, the average area in the statistics has suppressed the highlighted signal (Ullah et al., 2018). These responses of the precipitation events are possibly associated with the monsoons and western winds that are resulted in the summer and winter seasons, respectively (Bhatti et al., 2020).
Some of the recent studies have strong evidence for an increase in the precipitation regime (Ashiq et al., 2010), (Bhatti et al., 2020), (Ullah et al., 2018). The observed increase is generally linked to the frequency and intensity increases of extreme precipitation events, which are generally responsible for severe flooding in the study area (Khan et al., 2011). Similar events have been observed over a long time in Pakistan, which has caused severe damages to agriculture, civil and hydro-logical cycles, as well as living beings (You et al., 2017). Another limitation is the uncertainty of the data since the station data are usually subjected to the application of the synoptic-scale and recording capabilities are currently related to deviations and therefore could be identified in some other studies (Ullah et al., 2019), (Iqbal and Athar, 2018). Therefore, detailed findings with recent methods, simulations and projections must be adopted as an alternative approach to the better understanding of the precipitation nature at the regional level (Iqbal and Athar, 2018), (Ahmed et al., 2019). The linear regression of the various precipitation indices applied in the study shows that

rainy days are subjected to the general trend, increasing with slope and regression coefficient equal to 0.059. There was also a great variability throughout the study period, which is dominant with peaks and troughs indicating wet or dry events in the area (Bhatti et al., 2020). The heavy, very heavy, and extremely heavy rain events seemed to follow similar patterns to those observed for daily precipitation, where an increase in the trend and sizes of regression are of 0.017, 0.027 and 0.005, respectively. This increase in trend can be concluded by focusing on agriculture, where it can increase the yield of crops and vegetation in the study region, which consists mainly of arid and semi-arid regions with scarce vegetation. However, intense, very intense, and extreme intense events can affect the livelihoods of the community, already threatened by the dangers of flooding. The indirect effects of these events also occur in areas downstream of the Indus basin with some direct or indirect losses due to water stagnation, soil degradation and the deposition of carried sediments (Hassan and Ansari, 2015), (Khan et al., 2011).

The time-scale variability in precipitation indices peaked in the early 1990s, followed by decreasing in 2000-2005 and then increasing steadily in subsequent years. The total annual precipitation and the mean precipitation wet days have also been increased along with the coefficients of regression for about 0.62 and 0.054, respectively (Bhatti et al., 2020). However, the increase in total precipitation over the mean precipitation was more significant on rainy days, suggesting a higher precipitation value on the annual scale is linked to extreme events. The precipitation extremes percentiles showed an increasing trend with the coefficients of regression equal to 0.046 and 0.019 for the precipitation events of the 95^{th} and 99^{th} percentiles, respectively (Bhatti et al., 2020). The droughts of the late 1990s and early 2000s are also evident across all precipitation indices, particularly at the extremes of 95^{th} and 99^{th} percentiles. From these results, we can deduce that the total frequency and the amount of extreme rainfall continually increased during the period of 1980 to 2016 (Bhatti et al., 2020). The most significant increase has been observed for average annual precipitation on rainy days. The linear regression results were seen different than the SqMK test, which showed a decrease on some indices. On the other hand, increase at extreme rates, particularly after 2000, concluded that extreme events could occur more in Pakistan (Bhatti et al., 2020).

The increase has been noted in recent years and, therefore, must be considered for decisions at a regional level that related to a disaster, floods, food security, risk and vulnerability. The associated changes with the underlying dynamics in extreme events of precipitation could be due to the large-scale oceanic and atmospheric factors that have been examined in similar studies for the region (Gadiwala and Burke, 2019), (Galarneau et al., 2012), (Rasmussen et al., 2015). The results are associated with the latest trend prompted by climate change, as shown in the IPCC assessment reports (Stocker et al., 2013). The estimated linear trend of the extreme precipitation indices at an altitude of the study region highlighted there is a large variation in precipitation across the region of interest having altitude, it can therefore also be called a variation of latitude. The results suggest that humid days increases slightly with altitude, suggesting an increase in precipitation from the south heading to the north (Bhatti et al., 2020).

Typically, there are two dominants of winter precipitation in the central and eastern part of the study region, associated with western shocks and South-Asian

monsoon precipitation (Ullah et al., 2019). This is indicated by a tendency to increase precipitation at the latitude/altitude in the northern and western parts of the region, which become relatively wet than the rest of the region (Ashiq et al., 2010) which may be associated with an increase in westerly winds and monsoon.

For severe and very severe precipitation events, a slight decrease in amplitude through elevation is evident, indicating severe precipitation events in flat valleys and the decline in wet/dry high-altitude areas. Severe p events are observed to be in decreases with height. However, there are some seasons in the mid-altitude of the monsoon regions, where stations indicate an increasing trend. This suggests that the central regions are prone to these changes are faster in other parts of the region, such as the east and south-east regions that typically receive more, or less than 60% rainfall in the monsoon seasons. Overall, severe events tend to decrease from arid and semi-arid regions in the south up to the northern parts. The daily mean precipitation and the total annual precipitation slightly decreased, and with the mid altitude, it is slightly increased and then a decline in the high altitude. The precipitation extremes for percentiles of 95^{th} and 99^{th} also exert concurrently an increase in latitude, with an increase in the low-altitude coastal regions and then a decrease in the central dry valleys and a slight decrease in the rest of the area (Bhatti et al., 2020).

The frequency of the precipitation from the south to north, have been decreased in the south and increased in the northern regions of the country, which also have presented in some studies (Ullah et al., 2018), (Iqbal and Athar, 2018). Increased extreme events of precipitation can be observed from south to north, which suggests that the region has experienced an increase in the north of the country. The frequency is getting heavier in the same period, where precipitation has been increased in the arid regions in the south of the country. The study results are compatible with the recent global warming trends in the region, and related changes have also been predicted in AR5 by the IPCC (Stocker et al., 2013), (Ullah et al., 2019), (Ahmed et al., 2019).

The water cycle is also expected to change, which is required to be addressed in future planning of the water resources in the region (Ullah et al., 2018), (Ullah et al., 2019), (Mahmood and Jia, 2016). However, more depth studies can investigate models in a specific way. Extreme precipitation events have risen recently and are expected to increase soon. Intense and frequent precipitation extremes can enhance the risks connected and vulnerability to river or flash floods that can exponentially expose vulnerable regions worldwide. Pakistan is among the vulnerable regions due to the precipitation extremes caused by climate change (Cheng et al., 2012), recently its local water cycle has been affected severely. Furthermore, the seasonal diversity of precipitation along the latitude and longitude and the perennial flow pattern should have strongly influenced the local and remote flora and fauna. The limitations and vulnerabilities in the present study was designed to evaluate changes in extreme precipitation events based on selected extreme indices in the target region between 1980 and 2016 (Bhatti et al., 2020).

All the changes of the precipitation and water cycle in the areas might relate to an increase in the temperature of the air, which increases the holding of water capacity in the air generates more vapours. This holding capacity of water in the atmosphere has been raised by 7% because of the variations in the total temperature, as indicated by Trenberth and Fasullo (2012), that can explain

the observed higher precipitation. Events of precipitation with a magnitude of 50 mm showed a small decline in some regions of Pakistan, but in general the decline was not so evident, except in the north of the country. The sea surface temperature increase could also influence the evidence for an increasing trend of these indices (Bhatti et al., 2020). These mixed behaviours could be caused by the variable geographic locations of the regions as Pakistan highlights the limit of these influences (Ullah et al., 2019), (Iqbal and Athar, 2018). For the two precipitation seasons, a clear model cannot be observed throughout the region. For the remaining indices of precipitation, the core Indus basin increase, and the decline was significant in the central-western and central monsoon disturbance zones, excluding for the 99^{th} percentile. One possible reason could be the two different aspects of the region that includes dryness of the region and the moisture source precipitation. The drought in the region is predominantly arid to semi-arid and extremely arid (Ullah et al., 2019), (Haider and Adnan, 2014). The appearance of precipitation mainly leads to higher infiltration and lower runoff. With low runoff, evaporation and recycling amount of moisture through evaporation, transpiration is less and therefore less water is recycled (Galarneau et al., 2012). The second reason can be explained by the humid locations of the two precipitation modes that control the water cycle in the region. The twist could be reversed, and there are disturbances about possible changes in the track of the monsoons and the westerly winds (Dimri et al., 2015). The source of humidity in the summer comes from the Indian Ocean, while for the winter, it comes from the Mediterranean area. The variation in the path of the humid pattern can change the maxima of precipitation and therefore shift the precipitation (Bhatti et al., 2020).

Sarfaraz et al. (2014) showed the spatial distribution of normal annual and seasonal rainfall all over Pakistan, where he attributed in his findings surprisingly massive changes from north to south and presented that the sub-northern area of Pakistan has the highest yearly rainfall, i.e. from 1485-1775 mm. It decreases as it moves south, reaching its minimum range of approximately 37-327 mm in Balochistan, Sindh, and southern Punjab. Obviously, the inter-regional variability of precipitation (1738 mm) in the spatial distribution of normal annual precipitation indicates the steep climatic gradient over Pakistan. The distribution of rainfall during the summer monsoon in various sub-regions of Pakistan has also been observed, where it can be concluded that most of the precipitation concentration is in the sub-north areas of Pakistan (642-771 mm) surrounding the areas of Islamabad, Sialkot, Kakul, Balakot and the suburbs. The following elevated range, i.e. 514-642mm, cover the rest of the northeastern areas, which includes the areas of Jhelum, Kotli, Garhi Dupatta and Kamra stations (Sarfaraz et al., 2014). The upper third zone of 386-514 mm includes the area extending from Lahore in the northwest, followed by precipitation decrease in the south and southwest, to almost all of Balochistan (except some places in the northeastern region), southwest of Punjab, and central and upper regions of Sindh, where a minimum range of precipitation, i.e., 129 mm have been observed. From this, we can conclude that most of the monsoons fell in the sub-north regions of Pakistan. In terms of pattern, it is very similar to what has been defined in the spatial distribution of annual rainfall (Sarfaraz et al., 2014).

The spatial distribution of rainfall in Pakistan over a 30-year typical winter shows a wide range and is considered to be the second-highest, accounting for

30% of total rainfall. The largest precipitation range, 514-642 mm, is evident near Dir district in the northwest, followed by the second-highest range, 386-514 mm, which covers the areas of Murree, Kakul, Balakot, Saidu Sharif, and Garhi Dupatta. It's worth noting that the highest precipitation happens in the same geographic area (Sarfaraz et al., 2014). The minimal outreach is greater than three-quarters of Pakistan, extending from southwest to northeast, culminating around Mianwali and the perimeter, and reappearing on Gilgit-Baltistan from east to northeast. This is in contrast to the lowest interval shown in the spatial distribution of yearly rainfall; in fact, due to cyclones extending east to mid-latitudes by western disturbance, the western and southwestern parts of the country receive the majority of the rainfall during the winter season. Altitude, mountain barriers, and land distribution all influence (Martyn, 1992). Precipitation, which is the second most important climatic component (Walterscheid, 2011).

Pakistan is bordered by the high Himalayan-Karakoram-Hindukush (HKH) mountains, which have a considerable impact on the climate of the region by altering not only Pakistan's rainfall and temperature but also worldwide air circulation. In general, the wind-striking side of the mountainous region receives more precipitation in the subcontinent, whereas the opposite side, which lacks this benefit, has a parched appearance (Nasrullah, 1962). As a result, the great variety of precipitation observed in the annual and seasonal spatial distribution in Pakistan can undoubtedly be linked to the region's varied altitudes, unusual terrain, and mountain barriers. As a result, the large disparity in precipitation and temperature between southern and northern Pakistan turns out to be a crucial component in determining the many types of climates on Pakistan's mainland (Sarfaraz et al., 2014).

The diurnal climatological anomalies are the large-scale composite features of the 100 events with the highest standardized precipitation index from June to September. The combined average shows a southerly wind speed anomaly ranging from 450 to 200 hPa. The presence of southerly winds across northern Pakistan, which are part of a weak but spatially coherent wavy pattern that spans from north-eastern Europe to Japan, is the most remarkable evidence. This higher-level wind regime is very similar to what has been observed in earlier flood compositions and case studies in this area (Houze et al., 2011).

In the overall composition of the column water anomaly, Pakistan and Northwest India have a significant positive anomaly. This might be due to the northwestern extension of the summer monsoon, providing a lot of moisture to an otherwise dry area. Combining this with the region's complicated orography and a typical south winds, it's possible to deduce that the precipitation is partly attributable to the orography (Houze et al., 2011). Temperatures in the lower troposphere (900-800 hPa) have been found to be an effective predictor of wet thermodynamic activity in synoptic systems' tropics. The cold anomaly is widespread over Pakistan and neighbouring nations, with a magnitude of 22,000 in the centre. This deep cold anomaly is most likely the result of severe rainfall due to its prominent position alongside the general column water anomaly. There is a contrasting hot anomaly on the Tibetan plateau's east side, where the atmosphere is dry, and there is some decline (Hunt et al., 2018).

The analysis demonstrates the composite anomaly of the meridian wind speed at 450-200 hPa, in which a very evident wave pattern occurs after taking into account the synoptic situation of heavy rains in summer. Winds from the south

are three times stronger than in the summer over northern India, with relatively weak north winds over central China and the Gulf of Arabia. The wavelength of this wave train is about 5000 kilometres, or a planetary wavenumber of 6, which is out of phase with the Geo-potential anomaly concept. Because the geo-potential ranges from 450 to 200 hPa, the anomaly across Pakistan and Afghanistan is substantial. This depression is similar to that caused by a western transitory disorder in terms of intensity and duration (Hunt et al., 2018).
During the northern winter, western faults are known to move into this region, delivering considerable rainfall. Because the maximum humidity anomaly is towards the north-east of India, not far from the area of interest, there is a clear contrast between summer and winter anomalies. However, there is a positive humidity anomaly in northwestern India and Pakistan, where humidity stretches. Deep southerly tropospheric winds are required for this, which could be one cause for the excessive rainfall in the Himalayan foothills (Dimri, 2006). Finally, the temperature anomaly in the lower troposphere resembles its summer counterpart. At the foot of the Hindukush, an about 24k more robust cold anomaly has been discovered. On the east side of the Tibetan plateau, there is still a minor warm anomaly throughout much of central China. The closeness of summer and winter temperatures shows that these anomalies are caused directly by precipitation (Hunt et al., 2018).
Extreme circumstances at all degrees of latitude, particularly at wind or precipitation, are frequently attributed to synoptic or mesoscale occurrences. South Asia is divided into two seasons: in the winter, it is subjected to western disturbances (Dimri, 2006), and in the summer, it is subjected to low monsoon systems (Hurley and Boos, 2015). Despite the fact that their seasonal cycles are significantly controlled, both can occur out of season, and in the latter event, they are commonly referred to as tropical minima. In reality, Pakistan's devastating floods in 2010 were linked to a western disturbance and a monsoon depression (Houze et al., 2011). Both Pakistan and northwestern India contain large desert areas and upstream mountains that are prone to sudden heavy rain or high precipitation occurrences. The importance of mid and upper-troposphere dynamics as antecedents of summer floods is true in every season and pertains to winter floods. It has been established that in the case of extreme precipitation in the winter, the disturbance in the west is also linked to heavy rains (Hunt et al., 2018).

Table 3.1.1: Data Summary

Places	Minimum	1st Quartile	Median	Mean	3rd Quartile	Maximum
Barkhan	16	33.73	44.55	47.15	53.35	99
Jiwani	2	14.75	32	44.28	50.45	165
Khuzdar	15	30.1	38.1	43.33	45.35	223
Lasbella	8	28.73	38.6	48.23	48.4	269.6
Panjgur	6.1	15.25	23.6	27.25	36.25	64.5
Pasni	0	15.75	29.75	35.35	46	131.8
Zhob	10.1	28.25	35.3	37.7	41.62	120
Bunji	7.8	16.62	30.95	29.3	36.65	66.4
Cherat	35	41.75	49.5	63.92	73.5	257
Chillas	11.2	24.43	29.15	35.37	41.23	109.3
Chitral	23.4	35.7	41.5	51.43	57.52	161.2
DI Khan	21.1	45.15	52.85	59.09	66.7	150
Drosh	22	39.95	47.35	51.95	49.42	131
Gilgit	11	13.93	21.35	26.32	35.25	64.5
Lahore	29.4	58.75	78.8	87.61	113.47	189.7
Khanpur	4	17.77	35.6	48.39	63.25	173
Faisalabad	25	43.75	58.95	60.77	71	136
Sialkot	43	68.4	96.8	109.5	128.3	273.7
Jhelum	44	66.2	86.1	96.61	117.45	242.2
Badin	0	41.62	57.8	70.34	97.05	176.5
Chhor	2.3	41.17	60.5	71.28	90.85	214.6
Hyderabad	4	20.6	46.05	48.35	70.47	153
Jacobabad	3	15.8	41.6	58.83	57.08	323
Karachi	0	24.07	45.75	49.69	68.17	142.6
M-Daro	5	14.82	25.75	34.44	49.88	119.6
Nawabshah	0	19.38	29.6	42.95	65.65	143
Padidan	6	18.75	31.2	46.31	57.52	238
Rohri	5	18	37.5	46.76	63.3	173.7

3 Data & Methodology

3.1 Data

The data has been obtained from the Pakistan Meteorological Department, which consists of the annual maximum rainfall data from 1985 to 2016. The data has been recorded at 28 stations of different locations in Pakistan in millimetres (mm), however, the 28 stations do not cover entire Pakistan. The data has been divided into 4 different regions and contain 32 annual rainfall observations except for Nawabshah, where two values are missing for the year 2015 and 2016. The following table 3.1.1 will represent the important information of the data of the respective weather stations.
Table 3.1.1.
All these locations are highlighted in the following figure 3.1.1 in a map of Pakistan where the stations located are pointed by a black circle with a small dot. Most of the stations are situated in the south-west, which comes under the Province of Sindh. Balochistan is the largest province of Pakistan, which is

Figure 3.1.1: Map of Pakistan where all the 28 stations are highlighted by a black circle with a small dot

situated on southwest of the country, where most of the stations are scattered and distant from each other. Some of the stations are located in Punjab, which covers the central west of the country, while the northern most stations are located in the province of Khyber Pakhtunkhwa, including with the northern parts of Gilgit-Baltistan, which is an administrative territory.
The time series of each location is represented by the trend in the figures from 3.1.2 to 3.1.5 divided into four main regions where each station can be seen individually to understand the data pattern.

3.2 Methodology

To analyse our data, we will use the extreme value analysis for our results since our data contains the annual maximum value of precipitation therefore, we will adopt the block maxima approach to check the positive/negative trends maximum values. To check the above results, the model we are going to adopt is the generalized extreme value distribution model, which is further elaborated below. Furthermore, we will perform statistical tests to select the best fit model for our data. To check the best fit model, we will consider the AIC, BIC, to see the trend, we will calculate the tau (τ) and two-sided p-values through Mann-Kendall statistical test. The results are compared with the results of the Mann-Kendall test for monotonic trends.

3.3 Generalized Extreme Value

Suppose that $X_1, X_2, ..., X_n$ is a sequence of independent and identically distributed (IID) random variables with common distributed function F. To char-

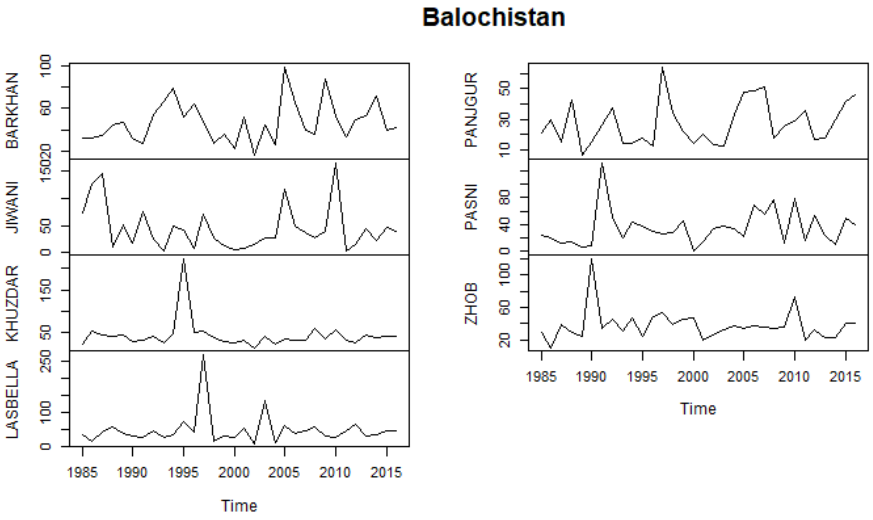

Figure 3.1.2: Time series data representation of stations in Baluchistan

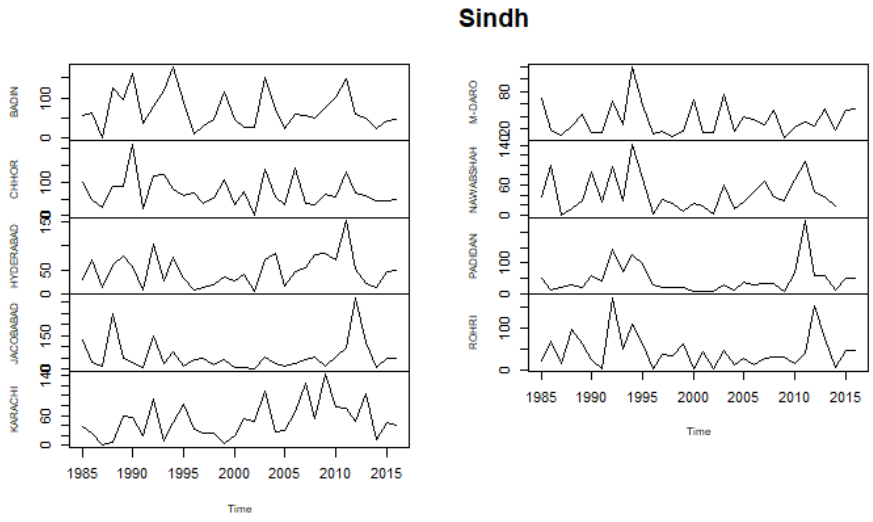

Figure 3.1.3: Time series data representation of stations in Sindh

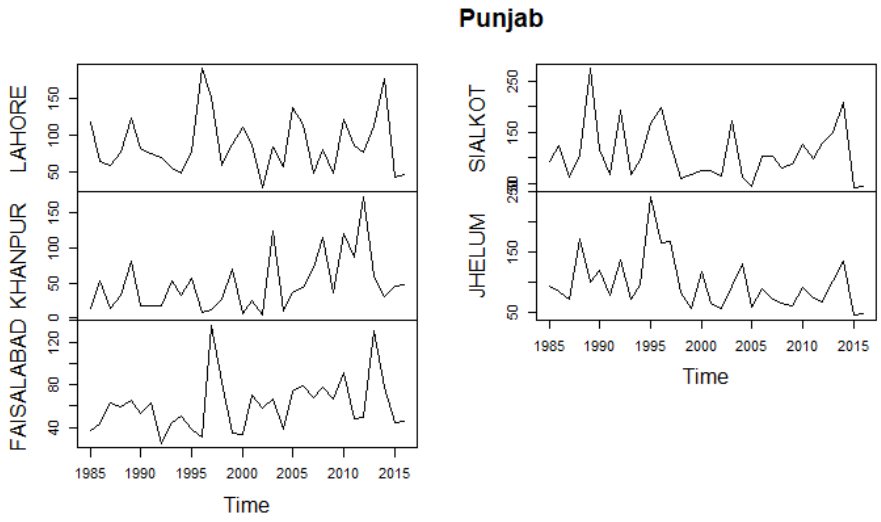

Figure 3.1.4: Time series data representation of stations in Punjab

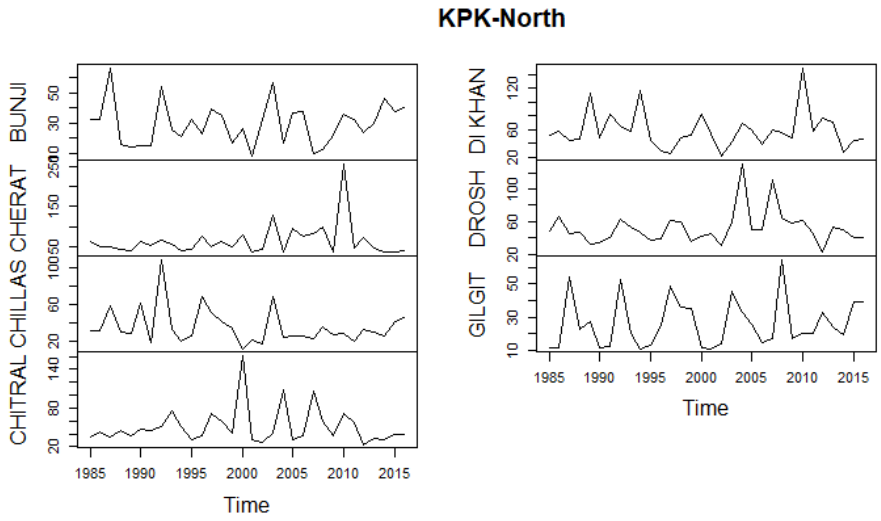

Figure 3.1.5: Time series data representation of stations in Khyber Pakhtunkhwa and North

acterize one way of extremes considering the distribution of maximum order statistic,

$$M_n = \max\{X_1, X_2, ..., X_n\}$$

The extremal types of theorem which is a result for the maximum M_n is analogous to the central limit theorem for the mean μ says that, if there exist sequences of constant $a_n > 0$ and b_n such that, as n $\to \infty$,

$$Pr\{(M_n - b_n)/a_n \leq x\} \to G(x)$$

For some non-degenerate distribution G, then G is of the same type as one of the following distributions:

$$I : G(x) = \exp - \exp(-x) \quad -\infty < x < \infty;$$

$$II : G(x) = \begin{cases} 0 & x \leq 0 \\ \exp(-x)^{-\xi} & x > 0, \xi > 0; \end{cases}$$

$$III : G(x) = \begin{cases} \exp\{-(-x)^{\xi} & x < 0, \xi > 0 \\ 1 & x \geq 0 \end{cases}$$

The three types of distribution, i.e., I, II and III are commonly known as Gumbel, Fréchet, and Weibull types, respectively and are also collectively known as Extreme Value Distributions (EVD). For Gumbel and Fréchet distributions, the limiting distribution G is unbound, which means the upper-endpoint tends to ∞. From these distributions, the Fréchet distribution gives heavier tails. However, for the Weibull distribution, the limiting distribution is bounded. In EVDs, there also exists a parameterisation that encompasses all three types of EVDs.
The Generalized extreme value distribution (GEV) often denoted $G(\mu, \sigma, \xi)$, with CDF:

$$G(x; \mu, \sigma, \xi) = \left\{ \exp\left\{ -\left[1 + \xi\left(\frac{x-\mu}{\sigma}\right)\right]_+^{-1/\xi} \right\}\right\}, \xi \neq 0$$

where $a_+ = max(0, a)$. the situation where $\xi = 0$ is not defined in above equation, but is taken as the limit as $\xi \to 0$, given by

$$G(x; \mu, \sigma) = \exp\left\{ -\exp\Big(-[(x-\mu)/\sigma] \Big)\right\}$$

For the parameter estimation to fit the GEV on the set of block maxima $M_{n,i}$, numerical maximum likelihood is the most common approach. By assuming independence, we can form the likelihood in the usual way:

$$L(\mu, \sigma, \xi) = \prod_{i=1}^{m} g(m_{n,i}; \mu, \sigma, \xi),$$

where g is the GEV probability density function and can be found after the differentiation of the distribution function of $G(x; \mu, \sigma, \xi)$, used before for the GEV. The probability density function g is therefore,

$$g(x;\mu,\sigma,\xi) = \left\{ \frac{1}{\sigma}\left[1+\xi\left(\frac{z-\mu}{\sigma}\right)\right]_+^{(-1/\xi)-1} \exp\left\{-\left[1+\xi\left(\frac{z-\mu}{\sigma}\right)\right]_+^{-1/\xi}\right\}\right\}, \xi \neq 0$$

Further, we will replace the parameters: $\mu, \sigma \quad and \quad \xi$ with their corresponding estimators $\hat{\mu}, \hat{\sigma} \quad and \quad \hat{\xi}$. Since there are no closed-form solutions for the GEV for their estimated parameters, the (log) likelihood cannot be solved analytically. Therefore, we can get this around by adopting a numerical method to obtain an approximate solution to use this problem. We will use R where it uses a Newton-Raphson type algorithm. As with all statistical models, there are various goodness-of-fit properties that would be considered to check the overall adequacy of the fitted GEV. Which includes probability plots, quantile-quantile (Q-Q plots) and density plots. While return level plots will be used to estimate the return level of estimated values.
Generalized extreme value distribution is normally fitted to time series on extreme values often used for the environmental data that referred to annual maxima of monthly or daily precipitation (Panagoulia et al., 2014). It was first found by Von Mises (1936) and later also independently noticed by meteorologist Jenkinson (1955).

3.4 Non-stationary Extremes

In the context of environmental processes, it is common to observe non-stationarity for the reasons that it possesses different seasons with different climate factors along with the long term trends evident in climate change. Allowing the GEV location parameter μ to change with time is one way to capture the trends observed. Simple linear trend in time seems plausible for the annual maximum data X_t we have used so that we could use the model as

$$X_t \sim GEV(\mu(t), \sigma, \xi),$$

where,

$$\mu(t) = \beta_\circ + \beta_1 t$$

where t is an indicator of year.
We can simply replace μ in the above expression with previous equation, giving the log-likelihood,

$$\begin{aligned} l(\beta_\circ, \beta_1, \sigma, \xi; x, t) &= -m\log\sigma - (1+1/\xi)\sum_{i=1}^{m}\log\left[1+\xi\left(\frac{x_i-(\beta_0+\beta_1 t_i)}{\sigma}\right)\right] \\ &\quad -\sum_{i=1}^{m}\left[1+\xi\left(\frac{x_i-(\beta_0+\beta_1 t_i)}{\sigma}\right)\right]_+^{-1/\xi} \end{aligned}$$

when,

$$\left[1+\xi\left\{\frac{x_i-(\beta_0+\beta_1 t_i)}{\sigma}\right\}\right] > 0, for \quad i = 1, ..., m$$

With the usual replacement when $\xi = 0$. We have used the R package (`extRemes`) for maximizing the log-likelihood which is discussed also in the appendices section.
For more details on the subject discussed in the above two sections, refer to the textbooks on Extreme Value Analysis: An Introduction to Statistical Modelling of Extreme Values by Coles (2001) which provides an accessible introduction to the topic for most audiences. For a more detailed explanation on the topic, see Statistics of Extremes: Theory and Applications by Beirlant et al. (2004).

3.5 Mann-Kendall Test

A Mann-Kendall trend test is adopted to determine the trend in the data set. It is a non-parametric test, where no underlying assumptions are made about the normality of the data. The null hypotheses (ho) if there is no trend in the data, and the alternative hypothesis can be defined as if there is a trend in the data. The trend can be either positive or negative, which totally depends on the p-value, and if the p-value of the test is below a certain level of significance which proves that there is statistically significant evidence, then it suggests that there is a trend in the data. The test was first suggested by Mann (1945), which has been widely used in environmental time series data.
The values in data are analysed as an orderly time series, where each value is compared to all the subsequent values. If we have multiple values of x, then $x_1, x_2, \ldots, x_n$ in the data where j in x_j represent the time, Mann-Kendall statistic can be calculated as:

$$S = \sum_{k=1}^{n-1} \sum_{j=k+1}^{n} \text{sign}(x_j - x_k)$$

The positive value of S indicates the positive trend where the negative value of S indicates the negative trend.

Table 4.0.1: Results Summary of Model fit 1(Stationary)

Places	Location SE ($\hat{\mu}$)	scale SE ($\hat{\sigma}$)	Shape SE ($\hat{\xi}$)	-Log Likelihood	**AIC**	**BIC**
Barkhan	2.953 (38.63)	2.15 (14.763)	0.137 (-0.003)	136.665	279.331	283.728
Jiwani	4.362 (22.398)	3.9 (20.511)	0.205 (0.395)	154.265	314.53	318.927
Khuzdar	2.245 (32.144)	1.745 (11.627)	0.103 (0.215)	132.677	271.355	275.752
Lasbella	3.447 (30.884)	2.768 (17.612)	0.122 (0.252)	146.85	299.701	304.098
Panjgur	2.147 (20.156)	1.682 (10.226)	0.184 (0.11)	127.079	260.159	264.556
Pasni	3.384 (22.851)	2.629 (16.775)	0.148 (0.15)	143.509	293.019	297.416
Zhob	2.317 (29.859)	1.661 (12.005)	0.095 (0.073)	130.983	267.967	272.364
Bunji	2.322 (23.2)	1.707 (11.399)	0.151 (-0.05)	127.566	261.132	265.53
Cherat	2.458 (45.246)	2.553 (11.539)	0.229 (0.642)	140.162	286.324	290.721
Chillas	2.136 (26.069)	1.716 (10.805)	0.135 (0.226)	130.89	267.781	272.178
Chitral	2.406 (37.998)	2.127 (12.084)	0.153 (0.373)	137.185	280.371	284.768
DI Khan	3.604 (47.087)	2.641 (18.326)	0.119 (0.072)	144.821	295.643	300.04
Drosh	2.518 (43.047)	1.834 (13.016)	0.101 (0.094)	134.12	274.24	278.637
Gilgit	2.024 (17.197)	1.912 (7.753)	0.355 (0.536)	125.243	256.487	260.884
Lahore	5.676 (69.344)	4.294 (27.904)	0.154 (0.073)	158.472	322.944	327.341
Khanpur	4.792 (26.672)	4.207 (21.92)	0.223 (0.357)	155.717	317.435	321.832
Faisalabad	3.562 (49.027)	2.686 (17.631)	0.145 (0.083)	143.884	293.768	298.166
Sialkot	7.264 (82.041)	5.846 (34.757)	0.181 (0.195)	167.681	341.363	345.76
Jhelum	5.34 (74.732)	4.358 (25.946)	0.17 (0.232)	158.986	323.972	328.369
Badin	7.71 (50.645)	5.797 (36.065)	0.175 (0.013)	155.299	316.598	320.801
Chhor	6.852 (52.346)	5.049 (33.236)	0.139 (0.039)	153.195	312.39	316.593
Hyderabad	5.693 (31.439)	4.518 (25.169)	0.218 (0.094)	145.842	297.685	301.889
Jacobabad	4.77 (22.039)	5.189 (21.62)	0.247 (0.718)	151.421	308.842	313.045
Karachi	5.925 (32.224)	4.597 (27.037)	0.195 (0.08)	147.786	301.572	305.776
M-Daro	2.769 (19.334)	2.527 (12.919)	0.197 (0.416)	131.138	268.276	272.48
Nawabshah	4.813 (24.743)	3.91 (22.338)	0.187 (0.216)	144.292	294.584	298.788
Padidan	3.958 (20.988)	3.958 (17.403)	0.256 (0.598)	142.908	291.816	296.02
Rohri	4.846 (24.562)	4.283 (21.477)	0.23 (0.376)	145.665	297.331	301.535

4 Results

In this section, we will discuss in detail the results of our analysis for the data of maximum value precipitation recorded in 28 different stations in Pakistan. The model results for our data is given in the following tables 4.0.1 and 4.0.2. Furthermore, from the two model results, the graphical presentation of the best fit model with better results of one station will be included in this section while the rest will be discussed verbally and graphical presentation of the remaining 27 stations for the same model are given in the section of Appendices at the end of the report.

In order to see the trend of the data, we have performed a statistical analysis of Mann-Kendall to check the positive or negative trend as discussed in the methodology in the following table4.0.3. According to the results, Khanpur and Karachi are the only two shares the high positive value, which shows the upward trend with strong statistical significance.

Table 4.0.2: Results Summary Model fit 2 (Non-stationary)

Places	Location $\beta_0, \quad \beta_1$	Scale $(\hat{\sigma})$	Shape $(\hat{\xi})$	-Log Likelihood	**AIC**	**BIC**
Barkhan	37.818, 0.0004	14.81	-0.005	136.664	281.3291	287.192
Jiwani	23.224, -0.0004	20.503	0.395	154.265	316.53	322.393
Khuzdar	31.147, 0.0005	11.637	0.215	132.677	273.354	279.217
Lasbella	29.496, 0.0007	17.636	0.252	146.849	301.699	307.562
Panjgur	-9.176, 0.014	10.237	0.111	126.947	261.895	267.758
Pasni	22.484, 0.0001	16.782	0.149	143.509	295.018	300.881
Zhob	22.404, 0.003	11.97	0.073	130.968	269.937	275.8
Bunji	23.116, 0.00005	11.416	-0.051	127.566	263.132	268.995
Cherat	46.067, -0.0004	11.522	0.643	140.158	288.316	294.179
Chillas	25.548, 0.0002	10.801	0.226	130.89	269.781	275.644
Chitral	41.002, -0.001	12.075	0.377	137.171	282.343	288.206
DI Khan	46.281, 0.0004	18.326	0.072	144.822	297.644	303.507
Drosh	42.42, 0.0003	13.017	0.094	134.121	276.242	282.105
Gilgit	18.726, -0.0007	7.787	0.530	125.256	258.512	264.375
Lahore	68.855, 0.0002	27.874	0.074	158.472	324.944	330.807
Khanpur	27.96, -0.0006	21.949	0.357	155.719	319.439	325.302
Faisalabad	48.929, 0.00006	17.647	0.083	143.884	295.768	301.631
Sialkot	82.406, -0.0002	34.723	0.196	167.681	343.362	349.225
Jhelum	74.807, -0.00007	25.902	0.233	158.985	325.971	331.834
Badin	49.805, 0.0003	35.980	0.015	155.298	318.597	324.202
Chhor	51.352, 0.0005	33.247	0.039	153.195	314.39	319.995
Hyderabad	32.424, -0.0004	25.17	0.094	145.843	299.686	305.291
Jacobabad	24.219, -0.001	21.602	0.719	151.418	310.837	316.442
Karachi	32.239, 0.00001	27.042	0.08	147.786	303.572	309.177
M-Daro	20.176, -0.0004	12.912	0.416	131.137	270.275	275.88
Nawabshah	24.978, -0.0001	22.349	0.215	144.292	296.585	302.19
Padidan	22.215, -0.0006	17.375	0.599	142.906	293.813	299.418
Rohri	25.501, -0.0004	21.473	0.376	145.665	299.331	304.935

Table 4.0.3: Data Trend

Places	$Tau(\tau)$	**2-sided p value**
Barkhan	0.145	0.249
Jiwani	-0.066	0.603
Khuzdar	-0.006	0.974
Lasbella	0.101	0.426
Panjgur	0.182	0.148
Pasni	0.188	0.135
Zhob	-0.01	0.948
Bunji	0.137	0.277
Cherat	-0.016	0.909
Chillas	-0.07	0.581
Chitral	-0.036	0.782
DI Khan	-0.02	0.883
Drosh	0.044	0.733
Gilgit	0.184	0.144
Lahore	-0.042	0.745
Khanpur	0.274	0.028
Faisalabad	0.208	0.098
Sialkot	-0.068	0.592
Jhelum	-0.254	0.042
Badin	-0.075	0.568
Chhor	-0.094	0.475
Hyderabad	0.08	0.544
Jacobabad	-0.011	0.943
Karachi	0.283	0.029
M-Daro	0.013	0.928
Nawabshah	0.048	0.721
padidan	0.013	0.928
Rohri	-0.082	0.532

4.1 Model Selection

In the GEV distribution model, we are focusing on the annual maxima, which in our case is the annual extreme precipitation from the period of 1985 to 2016. The two GEV models we have used, where model fit-1 is stationary and model fit-2 is non-stationary can be compared with the parameters criteria. By comparing the two models, the best model fit results according to AIC, BIC, standard error and log-likelihood values; model fit 1 (stationary) indicates the better significance of the results, and the model fit-2 (non-stationary) indicates higher uncertainty. Therefore, for the graphical representation, we will only consider Model fit 1, where we have neglected the location (μ) parameter changes with time and is considered as ~ 1.

4.2 Stationary Model

The model plot from the stationary GEV distribution fir for the station of Barkhan, also represented in figure 4.2.1, indicates the better goodness of fit on the QQ plot. However, the estimated ($\hat{\xi}$) value is negative, which suggest the heavier tail distribution. Apart from Barkhan, Bunji is another station, where the estimated shape ($\hat{\xi}$) value is negative affirms similar distributional significance.

Considering the data distribution of Barkhan, where the maximum value is 99, the estimated standard error values of Barkhan for all three parameters do not give the best significance. However, these values do not present higher uncertainty than some stations and lie almost on average. Thus, it could be concluded that for lower values, the model provides a good approximation. The value of AIC for Barkhan station is 279.331, which is the 8th lowest value and lies amongst the station, where the model fit indicates better significancy than most of the stations. The precipitation forecast is a bit of a challenge, especially for the extremes, but the consequences of the extremes can be higher. We cannot neglect the uncertainty at higher levels and for this station, as the return level is between 20 to 50 years for the highest value, which could bring alarming consequences, and the uncertainty could make it more severe than expected. The modelled and empirical quantiles on the QQ plot at higher-end distribution are drifting away from the goodness of fit at higher values that show the uncertainty of the data, which is also one of the challenges to assess certain data. The empirical density graph, too, is almost similar to model density and is skewed to the right, where the values get higher, which also suggests the uncertainty of the model only at higher values. Similar, description goes for the return levels, where the lower values are more likely to return more frequently, and the value, which is almost 100 mm, lies in between 20 to 50 years.

As far as the values presented in table 3.1.1, are concerned, Gilgit station, which is located in the north of Pakistan, has the least maximum value of precipitation of 64.5, which is similar to the Panjgur shows the best model fit amongst all the stations. The QQ plot presents the normal distribution of the data along with the density plot, where values estimated are close to the data distribution. The smaller values present better results, and as the value gets higher and the residual tends to get uncertain from the goodness of fit line. The density plot is rightly skewed and shows similar observations of QQ smoothness. The return level offers the accuracy where the extreme event is likely to occur between 20

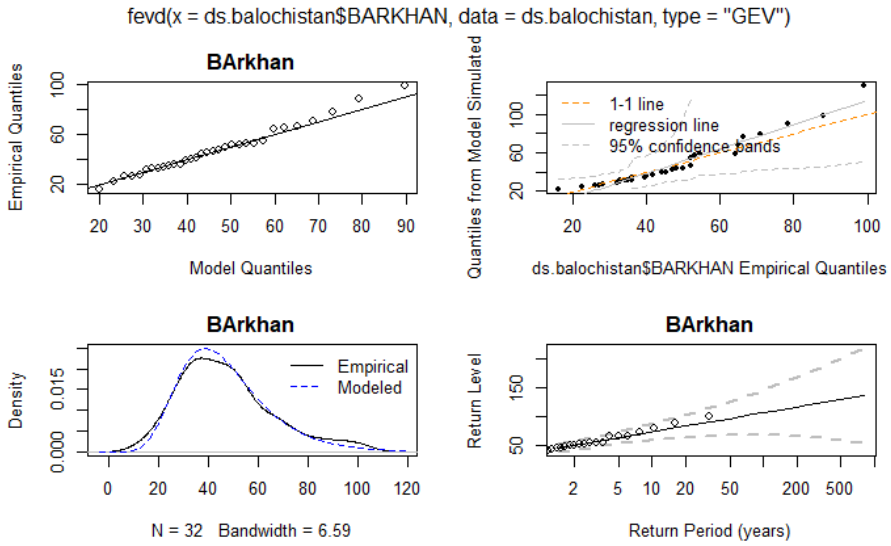

Figure 4.2.1: Model Plot for the station at Barkhan,Balochistan

to 50 years. Moreover, the trend is not much apparent, and it follows a similar pattern presented in the data, which is almost the uniform distribution.
If we compare the model results for Panjgur, which has the same least maximum, the model fit is not as good as Gilgit. It could be due to the reason that Panjgur has the lower minimum; however, if we neglect the AIC value, the standard error for scale and shape parameters has lower values for Panjgur, which is 1.682 and 0.184, respectively. For Gilgit, this figure is 1.912 and 0.355. While the negative log-likelihood, AIC and BIC suggest the better model fit for Gilgit, the lower bound tail of quantiles plot of Gilgit is better than Panjgur, and it shows a slight non-uniform pattern. If we consider the residuals, they are almost close to the smoothing line for Panjgur and not far, even for the higher values, indicating better goodness of fit. The return level shows a slightly different pattern, and the trend is somewhat increasing for 200 and 500 years.
The highest maximum value of precipitation, which is 323 mm, has been observed in Jacobabad, located in the southwest of Pakistan in the province of Sindh. The data also shows the high variation, and if we check the model value for the station, the AIC values are amongst the highest, including the standard error for the estimated parameter. The model density shows a higher peak than empirical density and is skewed to the right, indicating better estimation for smaller values. The return level for the highest value lies between 20 to 50 years, and it exceeds 500 mm after 100 years.
After Jacobabad: Khuzdar, Lasbella, Cherat, Jhelum, Sialkot and Padidan also show a high variation of data distribution where the maximum values are far greater than the mean value. As far as the model values among these regions, Khuzdar shows the better model fit results, and the return value of a maximum of 223 mm indicates that it lies between 20 to 50 years, yet it is far from the smoothing line. This could be due to the high variation is possess, and if we consider the 223 mm according to the model fit, the return level exceeds 1000

years.
If we consider the values for our model fit from 4.0.1, the worst performers according to the higher AIC values, the stations that represent worst model fit results are Sialkot, Jhelum, Lahore, Khanpur, Badin, Jiwani, Chhor, Jacobabad and Karachi, which are sorted respectively from highest to lower AIC values. Sialkot shows the highest value of AIC, lowest log-likelihood, the second-highest standard error value for a location and the highest for scale parameter; however, the standard error for shape parameter is not relatively high as compared to the other stations, which show a better model fit results. If we see the model graph, the values of empirical and modelled quantiles are dissociated with the lower end tail, and the dissociation goes up further on the higher end. The density for Sialkot is rightly skewed, and the return level for the maximum lies between 20 to 50 years. Nevertheless, the model return level shows a slight upward trend, and from 1 over 100 years, it could reach up to the maximum of an approximate 300 mm, and in 500 years, it could be even higher up to 500 mm.
The two biggest cities of Pakistan, i.e. Karachi and Lahore, are essential cities in terms of high population, urban structure and economy located in Sindh and Punjab provinces, respectively. If we compare these two cities, the standard error for the parameters of Lahore is better than Karachi. Still, the negative log-likelihood and AIC suggest a better model fit for Karachi. The quantile plot is better fitted for Karachi than Lahore, which also shows a similar trend with slightly higher values for Lahore; the density graph is rightly skewed for both the stations and the return level of the maximum precipitation, i.e. 142.6 mm and 189.7 mm is between 20 to 50 years for Karachi and Lahore, respectively. However, the model indicates that return level results can exceed 200 mm for Karachi and 300 mm for Lahore in 500 years.
A summary in table 4.0.1 of the estimates of the shape ($\hat{\xi}$) parameters of a GEV distribution for the series of the different stations. As you can see, most of the estimates are concentrated around zero with two stations with two negative values. The values are particularly interesting in relation to the station of Cherat having the highest value estimation and Bunji having the lowest value, while the standard error is 0.229 and 0.151, respectively. The tail distribution is limited to heavy tail and upper-bound tail distribution for Cherat and Bunji, respectively. Both of the stations are located in the north of Pakistan; hence it shows the high uncertainty in the distribution of the data.
Another important information if we consider the lowest standard error for shape parameter is Zhob which gives us the value as low as 0.095. The model fit plot shows us uniformity for all values where residuals are not much far from the fitted line except for the highest value of 120, which shows a significant variation and lie at a far distance. The return level for this value is from 20 to 50 years, but if we look at the model fit and derive the modelled value at the same return level, the value is less than 80. Similar behaviour has also been observed at Khuzdar station.
The use of extreme value theory in studying the trend on extreme precipitation represents a possible solution to the problems related to the GEV method. By focusing only on the study of the maxima, it is possible to explain only the functional form of the distribution's tails and, therefore, to grasp here values that would escape from traditional evaluations. Finally, it is always useful to remember that the models shown here do not produce values to be considered exact and faithful to what could happen.

5 Conclusion

It is very important to study precipitation extreme and to keep in mind its great consequences, which could result in a loss of human lives, urban infrastructure and ecological changes through urban flooding and water storms. Generalized extreme value is important to see the extreme considering high block maxima and forecasting similar events in return levels. AIC plays an important role in selecting the best model fit. Thus, it could be concluded that model fit 1, which do not estimate the prior location parameter and its change according to the time, shows better model fit results. The GEV and its distribution can also be implemented if we consider the block minima to study the dry events, which could also be implemented to understand and forecast harsh conditions.
The stations with high variations do not give us better model fit results. The quantiles plot shows that for high values, the model fit is uncertain for almost all the stations, and the residuals are drifting at higher upper-end tail distribution. In addition, virtually all the quantile plots show us the normal distribution with better model fits. The return level for the maximum extreme lies between 20 to 50 years except for a few, which include Zhob, Khuzdar and some other stations. The use of extreme value theory in studying the trend on extreme precipitation represents a possible solution to the problems related to the GEV method. By focusing only on the study of the maxima, it is possible to explain only the functional form of the distribution's tails and, therefore, to grasp here values that would escape from traditional evaluations. Finally, it is always helpful to remember that the models shown here do not produce values to be considered exact and faithful to what could happen in reality.
The annual maximum is only limited to a generalized extreme model with block maxima for 32 years periods. More data could also give us other alternative models, such as Generalized Pareto and maximum over the threshold. GEV on extreme precipitation can provide us with better insights to consider hazard and risk management control and deriving climate change policies.

Appendices

In this section, we will explain the R package `extRemes` used for modelling our data on extreme precipitation along with the work we have performed. Further, we will explain how to perform statistical analysis for the model we have used, and at the end of the section, we will include model plots for the remaining 27 stations, which have been discussed in the results section.

A extRemes

`extRemes` is a package we have used in R. It is a set of functions for performing extreme value analysis of a process to interest, either maximizing blocks over long blocks or overruns on a high threshold. The high threshold is another type of extreme value model generally known as Generalized Pareto (GP), used for large data sets containing monthly or daily information.

A.1 fevd

We have used the `fevd` function from the above package to fit our extreme precipitation distribution. It is also used to fit different univariate extreme value distribution functions such as Generalized extreme value (GEV), Generalized Pareto (GP) etc.

A.1.1 Usage

```
fevd(x, data, threshold = NULL, threshold.fun = ~1, location.fun = ~1,
scale.fun = ~1, shape.fun = ~1, use.phi = FALSE,
type = c("GEV", "GP", "PP", "Gumbel", "Exponential"),
method = c("MLE", "GMLE", "Bayesian", "Lmoments"), initial = NULL,
span, units = NULL, time.units = "days",
period.basis = "year", na.action = na.fail,
optim.args = NULL, priorFun = NULL, priorParams = NULL,
proposalFun = NULL, proposalParams = NULL, iter = 9999, weights = 1,
blocks = NULL, verbose = FALSE)
```

A.2 Output

Plot Character describing what texture is desired. Default is “primary”, which creates a 2 by 2 panel of plots containing: The QQ plot of the data quantiles versus fitted model quantiles (type “qq”), here the excellent fit will create a linear intercept of points on the line. Another QQ plot (“qq2”) similar to above is the plot of the quantiles of the model-simulated data versus the data, which also creates confidence bands and a regression line fitting the quantiles. Also, here, the excellent fit will create a linear intercept of points on the line.
A density plot of the data with the model fitted density (Density type) and,
A return value frame (type “rl”) is done on the log-scale for the abscissa where EVD can be understood by the shape, such as concave is for heavy tail, straight for a light tail and convex for the bounded upper tail. 95 percent CIs are also presented in grey dashed lines. In the case of non-stationary models, the data

are plotted as a line, and the "effective" return levels of 20-period and 100 annual periods. In the stationary (fixed) model, the return level presented show the return levels founded for the return periods specified by return.period, as well as the associated CIs (computed with standard method arguments) based on the estimation method used in the adjustment. For non-stationary models that the data is plotted as a line with associated actual performance levels for performance periods of 2, 20 and 100 years.
Other possible values for the type are "hist", which is similar to "density" but shows the histogram of the data.
The "trace" track offers a panel of graphs showing negative logarithmic probability and negative logarithmic probability of gradient for each of the estimated parameters; it also allows a parameter to vary by p range, while the others remain fixed at the estimated values. For the MLE method, probability traces are displayed for each parameter of the model, all but one parameter is fixed on the MLE values, and the negative log-likelihood is plotted for variable values of the parameter of interest. The negative logarithmic probabilities of the gradient are also given for each parameter. These are useful for diagnosing the adjustment problems that occur in practice. To facilitate interpretation, the gradients are displayed just below the probabilities of each parameter.

A.3 Other outputs

Likelihoods are proportional to probability densities or mass functions. For the probability probability densities or mass functions f $\{x, (\mu, \sigma, \xi)\}$, we can form the likelihood in a way that:

$$L(\mu, \sigma, \xi | x_1, .., x_m) = \prod_{i=1}^{m} f(x_i | \mu, \sigma, \xi),$$

where, x is the variable and (μ, σ, ξ) are the parameters, Given x, MLEs try to maximize the likelihood $L(\mu, \sigma, \xi)$ over all possible values of (μ, σ, ξ). We can use log-likelihood because where it converts products into sums and the natural logarithmic function is a monotone transformation. The above equation becomes,

$$\log L(\mu, \sigma, \xi | x_1, .., x_m) = \log \sum_{i=1}^{m} f(x_i | \mu, \sigma, \xi),$$

Where values closer to 0 indicate a better model fit pattern.

A.3.1 Estimated parameters

Estimated parameters are values of parameters for the distribution depending on the fit to the data.

A.3.2 Standard error (SE) estimates

Estimate the standard deviations for all the parameters.

A.3.3 Co-variance matrix of the estimated parameters

The variance of all the parameters on the diagonal; Co-variance between variables in other parts of the matrix. If the covariance values are significant, it indicates there is a dependency between the model parameters.

A.3.4 AIC (Akaike Information Criterion)

The parameter measures the relative quality of a model in statistics which consider the trade-off between model complexity and quality of goodness of fit.

$$AIC = 2p - 2\log(L)$$

Where p is the number of parameters, and L is the maximized value of the likelihood function. Comparing two models, a model with a lower AIC value is considered a "better" model.

A.3.5 BIC (Bayesian Information Criterion)

Similar to AIC, it is known to be,

$$BIC = p\log n - 2\log(L)$$

Where n is the number of data points, p is the number of parameters, and L is the maximized likelihood function value.

B Stationary model

In the stationary, we have selected all the parameters i.e., $(\mu, \sigma, \xi =\sim 1)$. Therefore, the fevd function for our model fit is,

```
fevd(x, data, type="GEV", method="MLE", shape.fun=~1,
location.fun=~1, scale.fun=~1, units="mm", main="station")
```

S3 method for class `fevd`

```
plot(x, type = c("primary", "probprob", "qq", "qq2",
"Zplot", "hist", "density", "rl", "trace"),
rperiods = c(2, 5, 10, 20, 50, 80, 100, 120, 200, 250, 300, 500, 800),
a = 0, hist.args = NULL, density.args = NULL, d = NULL, ...)
```

Note that the plot fit for the function argument used for fevd is shown in the title by default. If you assign the title as "main" in the argument, it can give the title individually for the graph presented in the plot.

B.1 Summary example

We have selected one station to present the summary results of the model here as an example where it can be seen in the figure B.1.1; also, all the results for the model fit are presented in table 4.0.1.
In the figure B.1.2, a panel of graphs showing negative logarithmic probability and negative logarithmic probability of gradient for each of the estimated

```
 Negative Log-Likelihood Value:  136.6655


 Estimated parameters:
    location        scale        shape
38.630915504 14.763639513 -0.003889362

 Standard Error Estimates:
 location     scale     shape
2.9539275 2.1503373 0.1370801

 Estimated parameter covariance matrix.
           location      scale       shape
location  8.7256879  2.4475673 -0.14918995
scale     2.4475673  4.6239507 -0.09194730
shape    -0.1491899 -0.0919473  0.01879095

 AIC = 279.3311

 BIC = 283.7283
```

Figure B.1.1: Model summary for the station at Barkhan, Balochistan

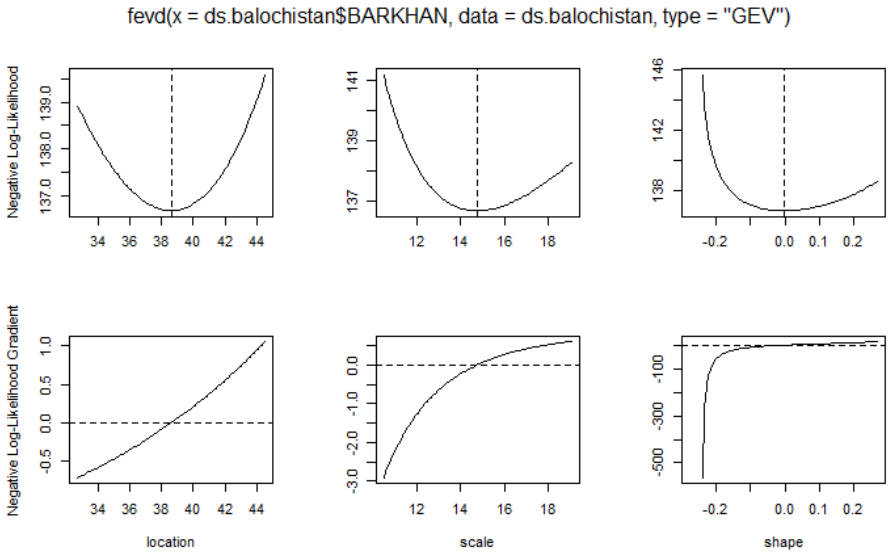

Figure B.1.2: Traces for the station at Barkhan, Balochistan

parameters which also have allowed a parameter to vary by p range, while the others remain fixed at the estimated values.
Here we have used the MLE method, where probability traces are displayed for each parameter of the model, where all but one parameter is fixed on the MLE values, and the negative log-likelihood (i.e. 136.665) is plotted for variable values of the parameter of interest. The the negative logarithmic probabilities of the gradient are also given for each parameter, including with the gradients, displayed just below the probabilities of each parameter where the adjustments required are suggested.
The probability plot is given in figure B.1.3 to assess the goodness of fit of probability distributions estimated. Here, the plot represents the significant goodness of fit, including the exponential trend of empirical probabilities versus the model probabilities.

B.2 Confidence Intervals and Return Level

In the table B.2.1, the values of the confidence interval and return level of 100 years are presented. CI is used to identify the uncertainty between the return level, which comes from the statistical variations. Here we have used a 95 % confidence interval which contains the lower and upper bound for the estimated range for the return level. From the CI and its return level results extracted from the stationary model, Jacobabad and Padidan, located in the province of Sindh, indicates a very high uncertainty. Jacobabad also has the highest extreme value for the 100 years return level, i.e. (811.626 mm), while Bunji has the lowest minimum value of 69.999 mm for extreme in a 100-year return level.

Table B.2.1: Confidence interval and return level

Places	95 % CI lower, upper	**100-year rl**
Barkhan	66.771, 145.112	105.942
Jiwani	-31.838, 612.128	290.145
Khuzdar	62.498, 184.790	123.664
Lasbella	67.236, 300.940	184.088
Panjgur	30.575, 132.383	81.480
Pasni	50.383, 217.704	134.044
Zhob	60.649, 95.531	130.411
Bunji	43.218, 96.779	69.999
Cherat	-134.336, 879.400	372.532
Chillas	44.507, 182.784	113.646
Chitral	40.312, 331.455	185.884
DI Khan	87.108, 207.306	147.208
Drosh	75.345, 160.684	118.015
Gilgit	-142.166, 488.365	173.100
Lahore	114.690, 329.334	222.012
Khanpur	-32.238, 598.675	283.219
Faisalabad	80.547, 215.420	147.984
Sialkot	106.724, 575.548	341.136
Jhelum	94.490, 482.311	288.401
Badin	99.621, 343.985	221.803
Chhor	113.681, 326.320	220.001
Hyderabad	42.871, 309.937	176.404
Jacobabad	-551.557, 2174.808	811.626
Karachi	56.604, 308.980	182.793
M-Daro	-16.974, 414.625	198.825
Nawabshah	31.991, 369.429	200.710
padidan	-254.045, 1149.688	447.821
Rohri	-52.819, 632.390	289.786

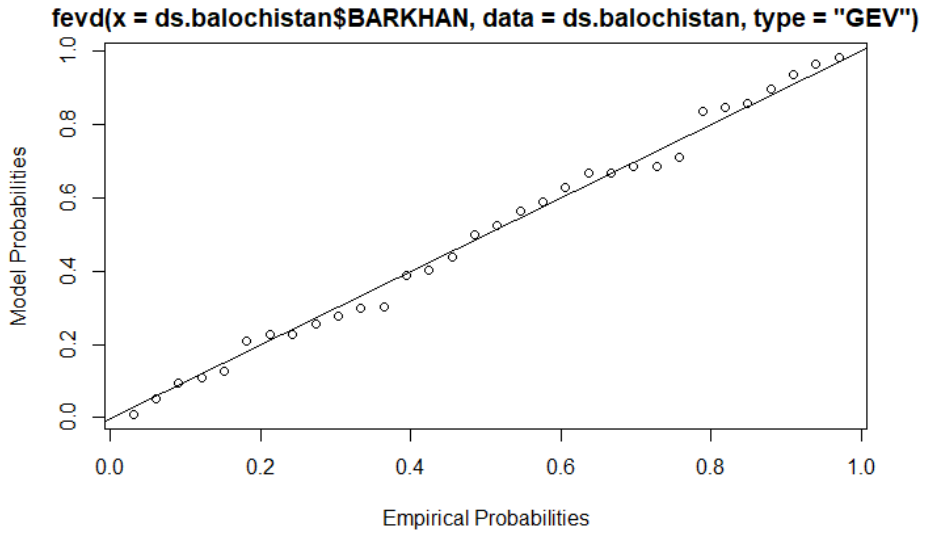

Figure B.1.3: Probability plot for the station at Barkhan, Balochistan

```
Negative Log-Likelihood Value:  136.6646


Estimated parameters:
          mu0           mu1         scale         shape
37.8181534132  0.0004274065 14.8105668441 -0.0053433542

AIC = 281.3291

BIC = 287.1921
```

Figure C.0.1: Model summary for the station at Barkhan, Balochistan

C Non-stationary model

In this model, we have allowed the GEV location parameter μ to change with the time to capture the trends observed. Therefore, the fevd function for this model fit is,

```
fevd(x, data, type="GEV", method="MLE", shape.fun=~1,
location.fun=~year, scale.fun=~1, units="mm", main="station")
```

We have not discussed this model based on the parameters used as a criterion to select a better model fit. However, the model information table has been included in the result section in table 4.0.2. The model summary result using one example is given in the figure C.0.1.

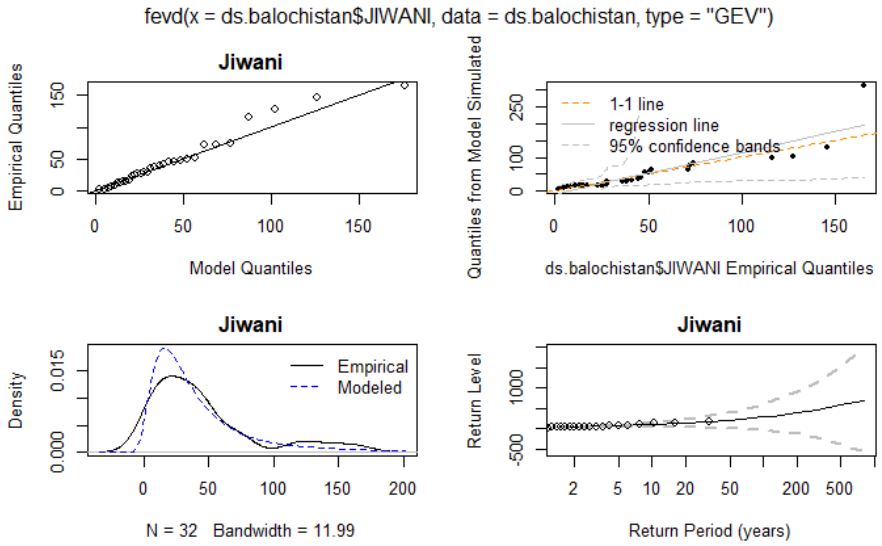

Figure D.0.1: Model Plot for the station at Jiwani, Balochistan

D Plots

In this section, we will present the remaining model plots of the 27 remaining stations from figure D.0.1 to D.0.27, as discussed in the methodology. The description and information of interest have also been discussed in the results section. However, the estimated shape value is ($\hat{\xi} < 0$) for the station of Barkhan and Bunji, therefore, we can limit the distribution as Weibull or bounded upper tail distribution. In comparison, the rest of the stations share the heavy tail distribution. The bounded tail distribution can be observed in return level in the model plots of the above-mentioned stations, which represent the slightly convex shape can be seen in 4.2.1 and D.0.7.

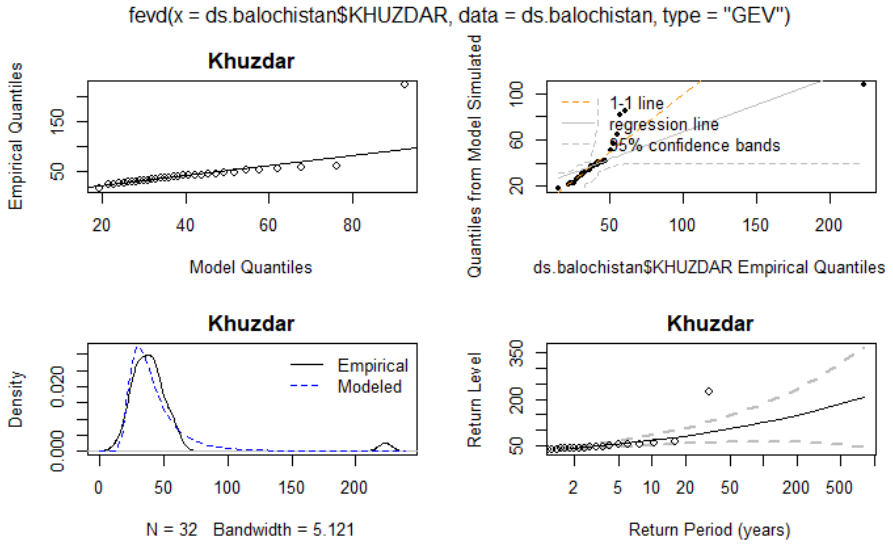

Figure D.0.2: Model Plot for the station at Khuzdar, Balochistan

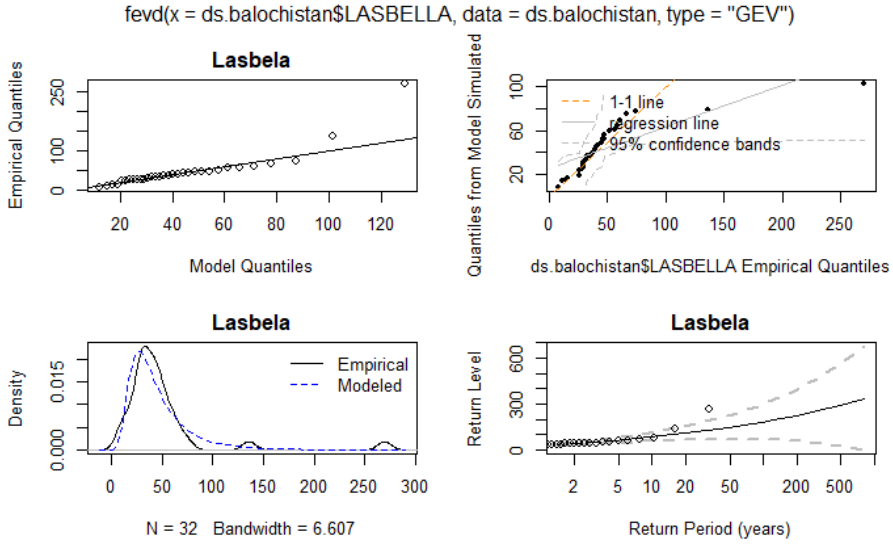

Figure D.0.3: Model Plot for the station at Lasbella, Balochistan

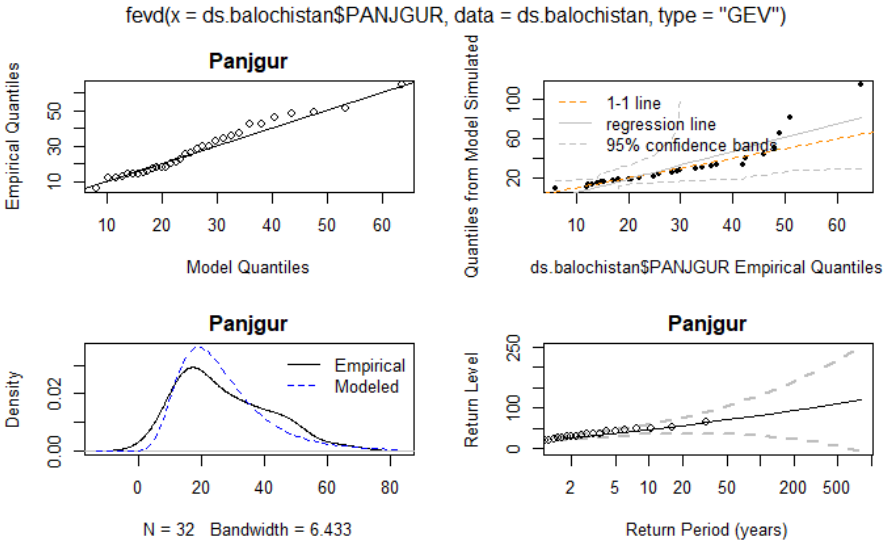

Figure D.0.4: Model Plot for the station at Panjgur, Balochistan

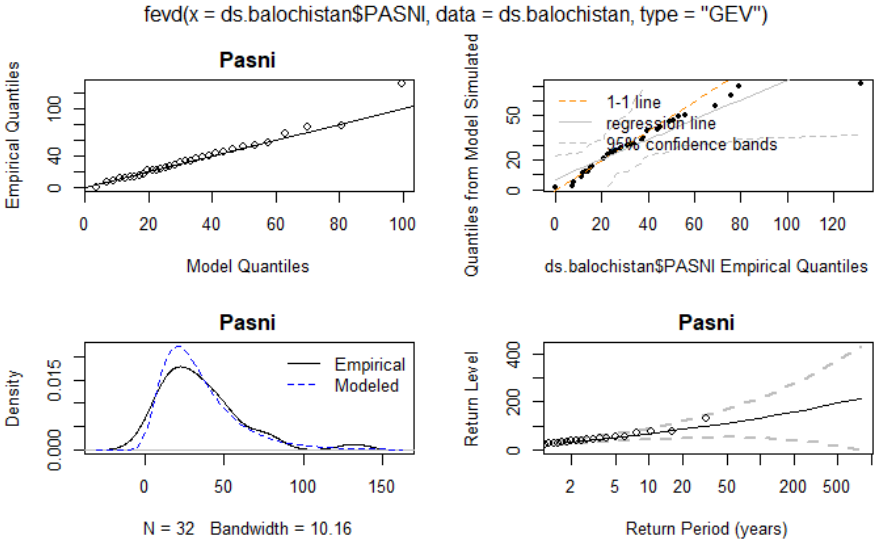

Figure D.0.5: Model Plot for the station at Pasni, Balochistan

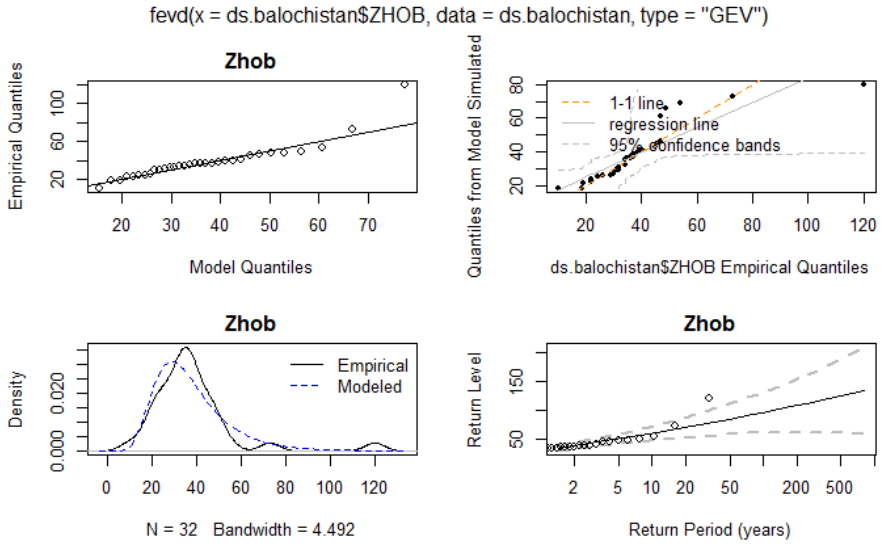

Figure D.0.6: Model Plot for the station at Zhob, Balochistan

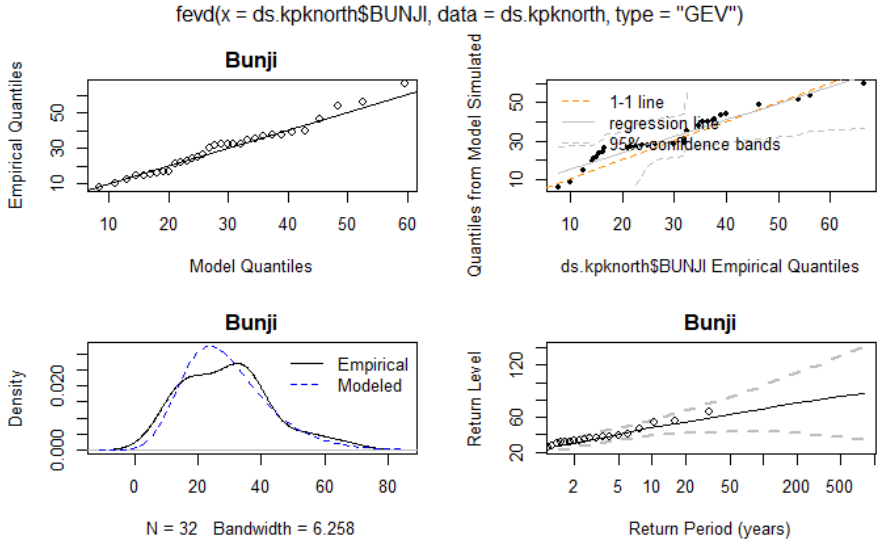

Figure D.0.7: Model Plot for the station at Bunji, Khyber Paktunkhwa/North

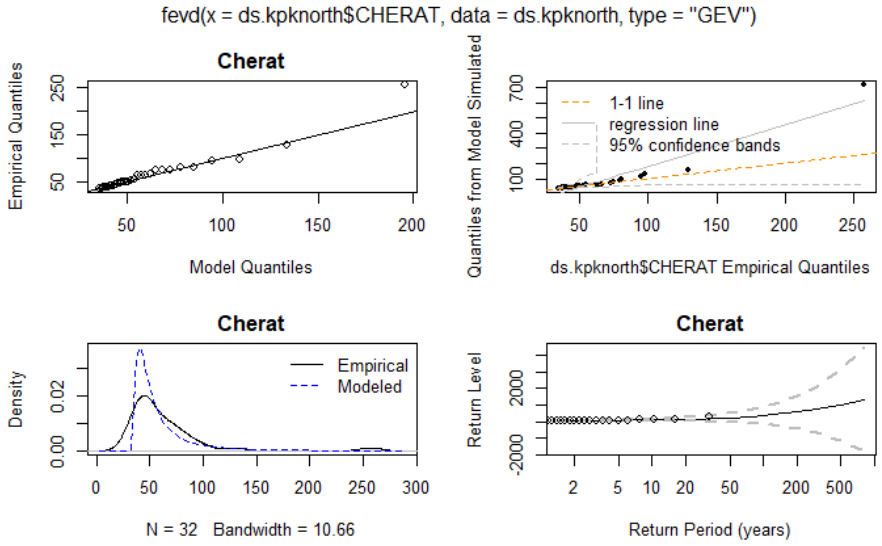

Figure D.0.8: Model Plot for the station at Cherat, Khyber Paktunkhwa/North

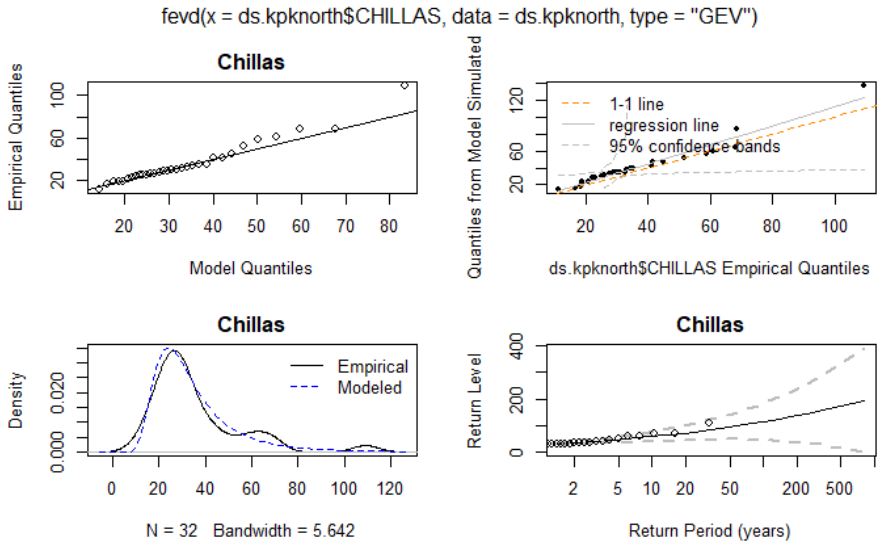

Figure D.0.9: Model Plot for the station at Chillas, Khyber Paktunkhwa/North

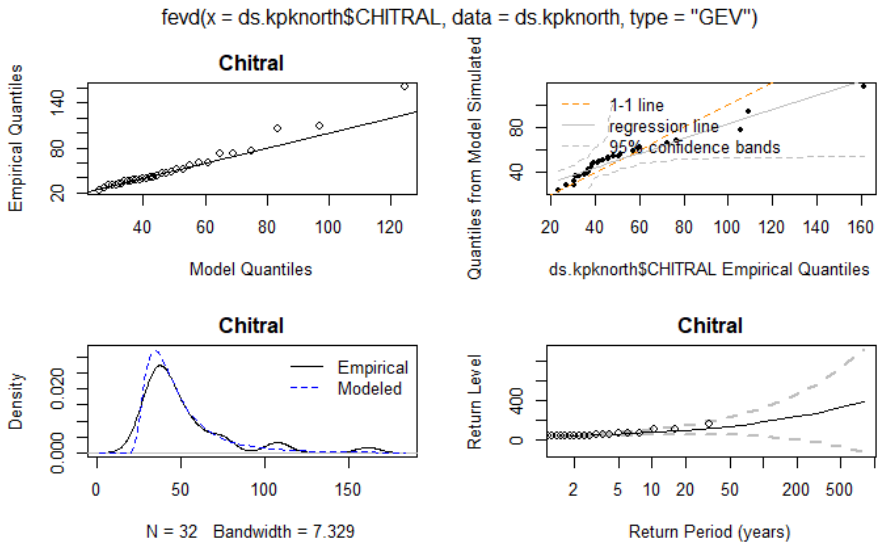

Figure D.0.10: Model Plot for the station at Chitral, Khyber Pakhtunkhwa/North

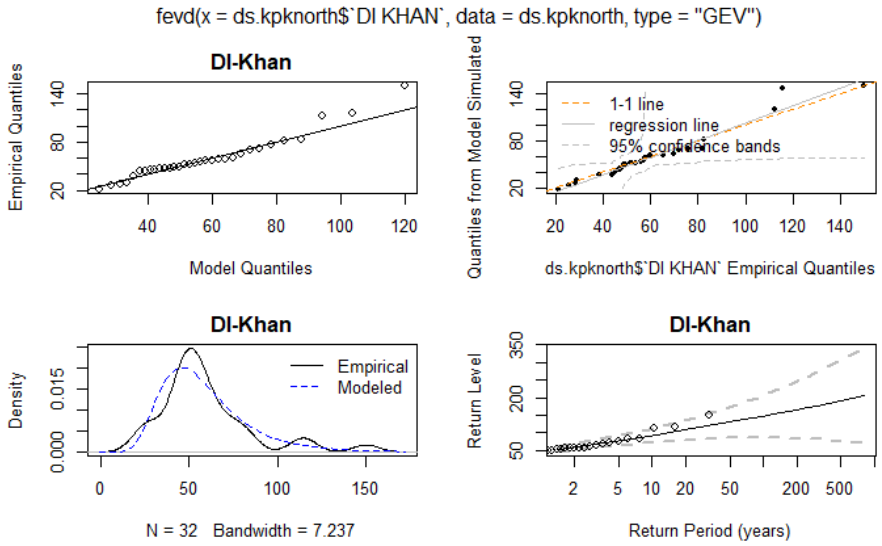

Figure D.0.11: Model Plot for the station at Dera Ismail Khan, Khyber Pakhtunkhwa/North

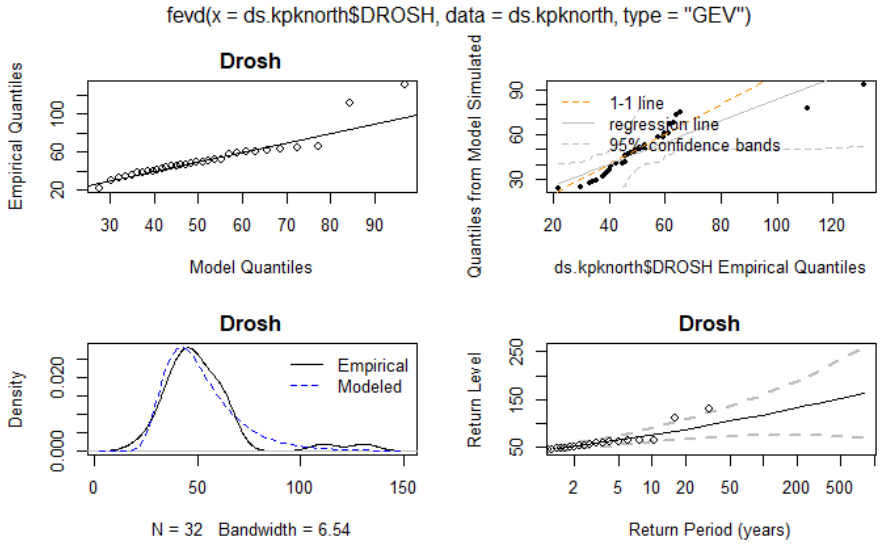

Figure D.0.12: Model Plot for the station at Drosh, Khyber Paktunkhwa/North

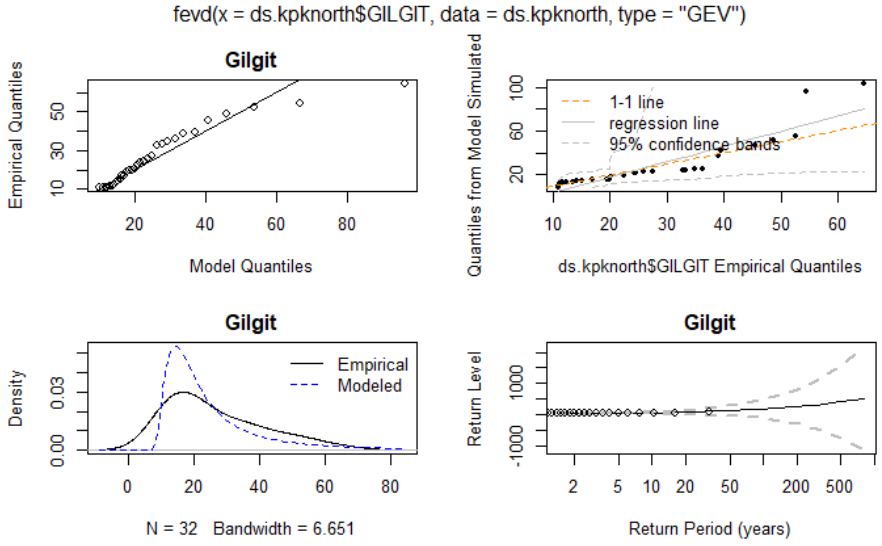

Figure D.0.13: Model Plot for the station at Gilgit, Khyber Paktunkhwa/North

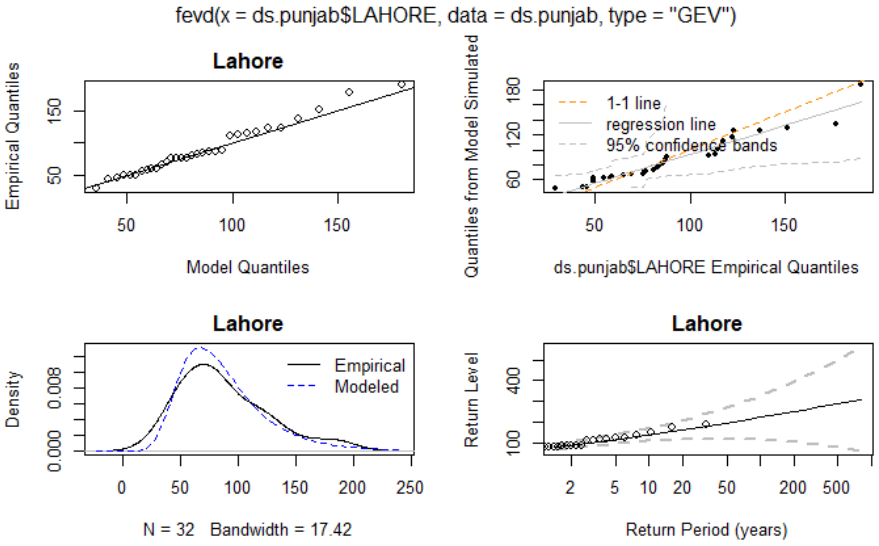

Figure D.0.14: Model Plot for the station at Lahore, Punjab

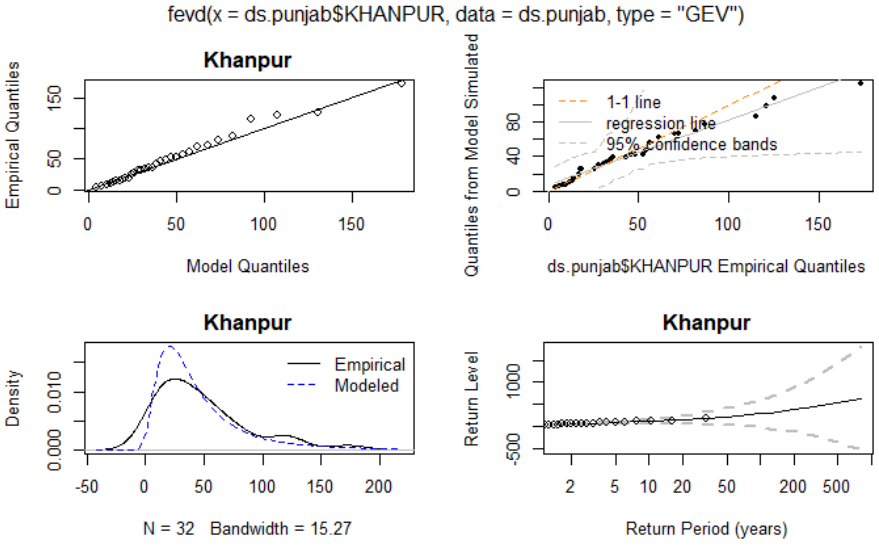

Figure D.0.15: Model Plot for the station at Khanpur, Punjab

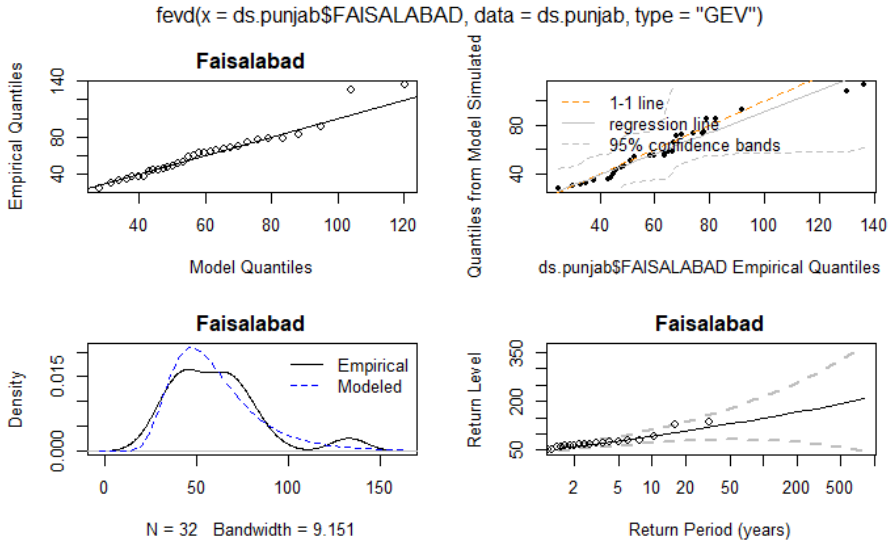

Figure D.0.16: Model Plot for the station at Faisalabad, Punjab

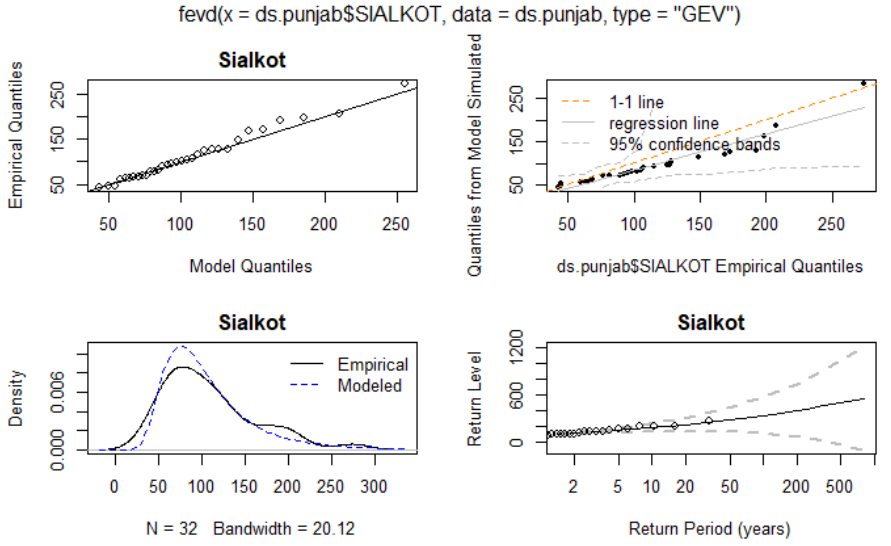

Figure D.0.17: Model Plot for the station at Sialkot, Punjab

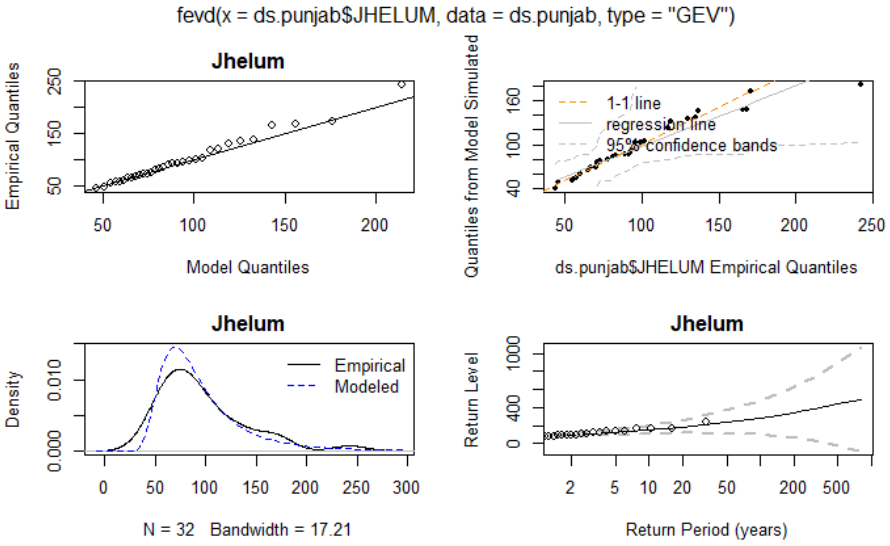

Figure D.0.18: Model Plot for the station at Jhelum, Punjab

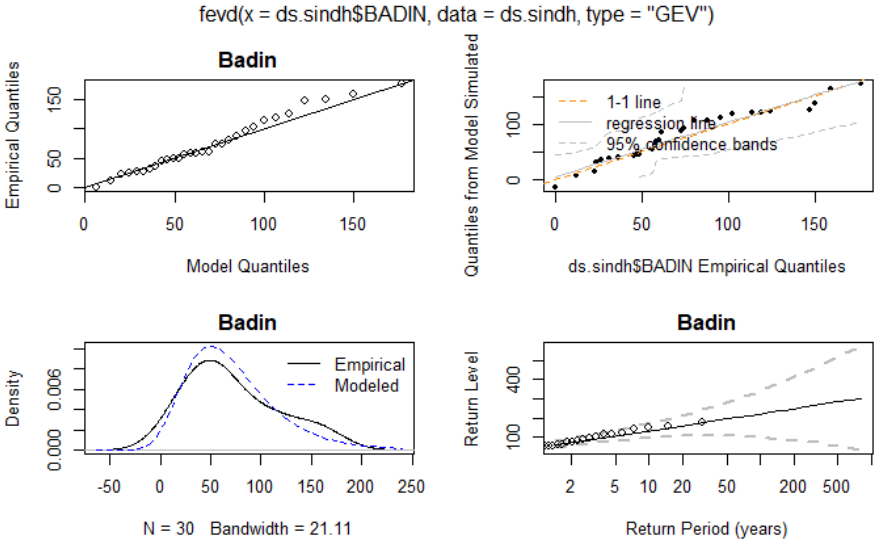

Figure D.0.19: Model Plot for the station at Badin, Sindh

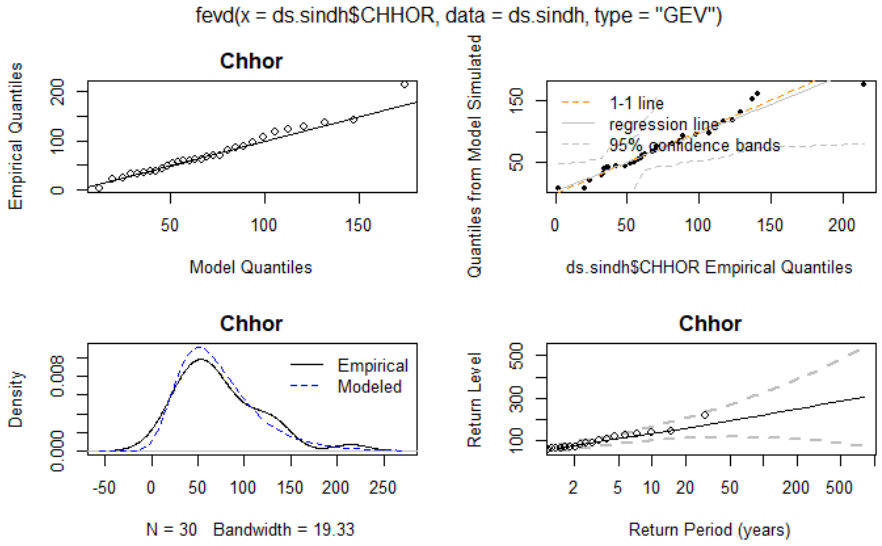

Figure D.0.20: Model Plot for the station at Chhor, Sindh

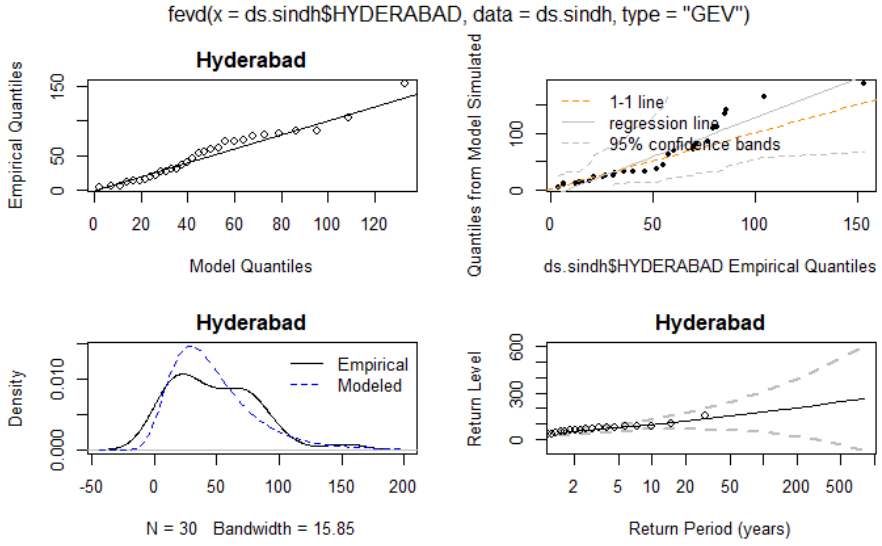

Figure D.0.21: Model Plot for the station at Hyderabad, Sindh

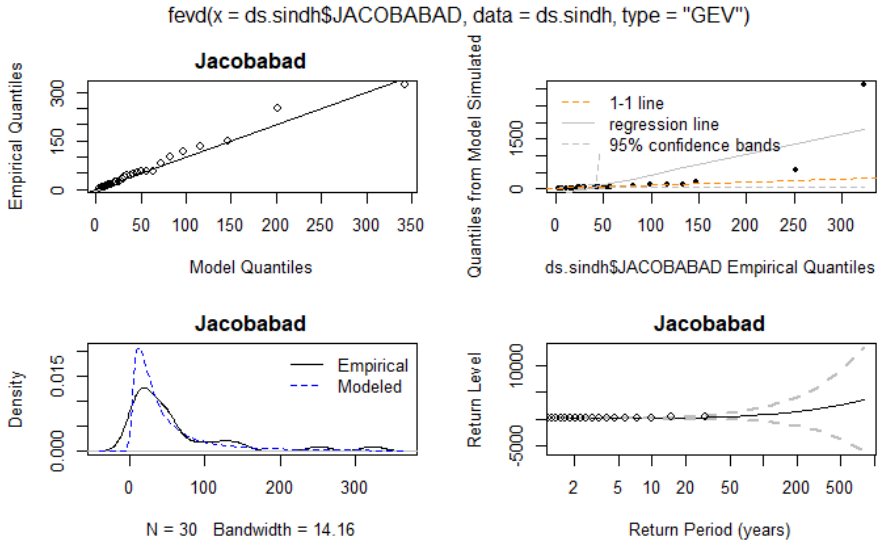

Figure D.0.22: Model Plot for the station at Jacobabad, Sindh

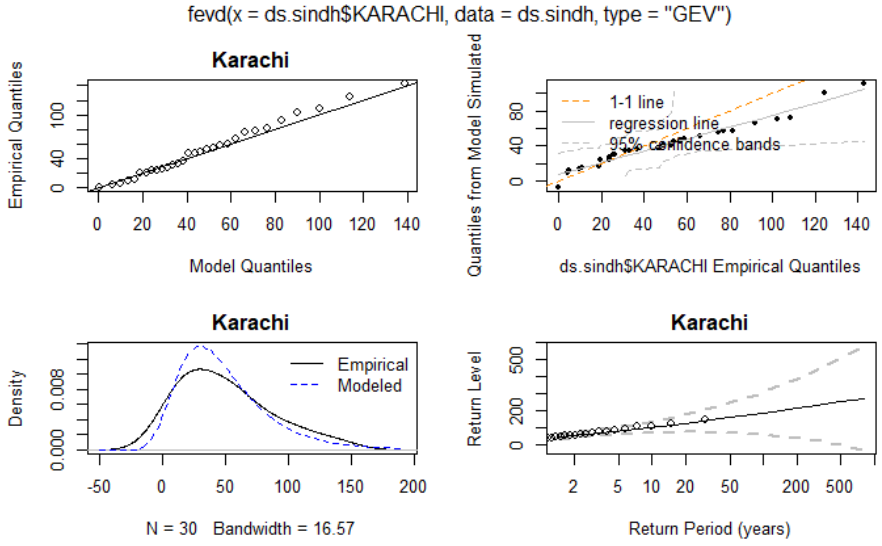

Figure D.0.23: Model Plot for the station at Karachi, Sindh

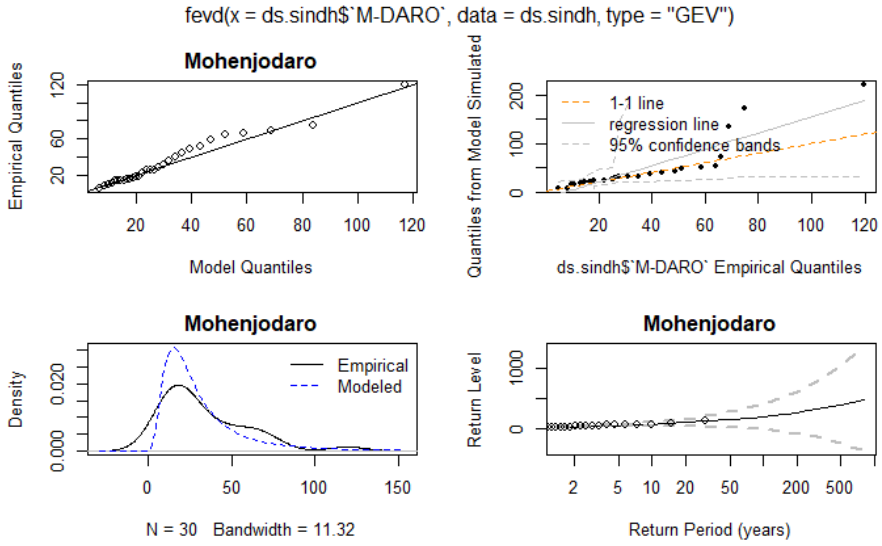

Figure D.0.24: Model Plot for the station at Mohenjo Daro, Sindh

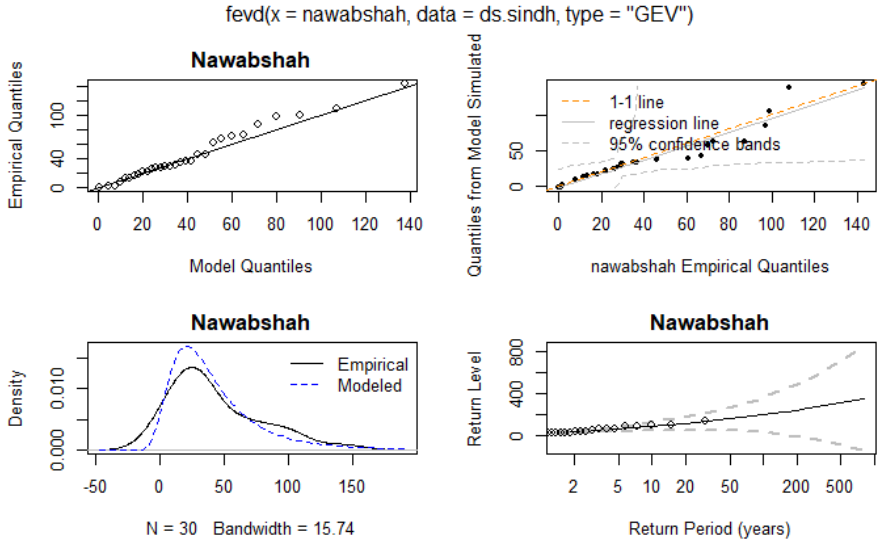

Figure D.0.25: Model Plot for the station at Nawabshah, Sindh

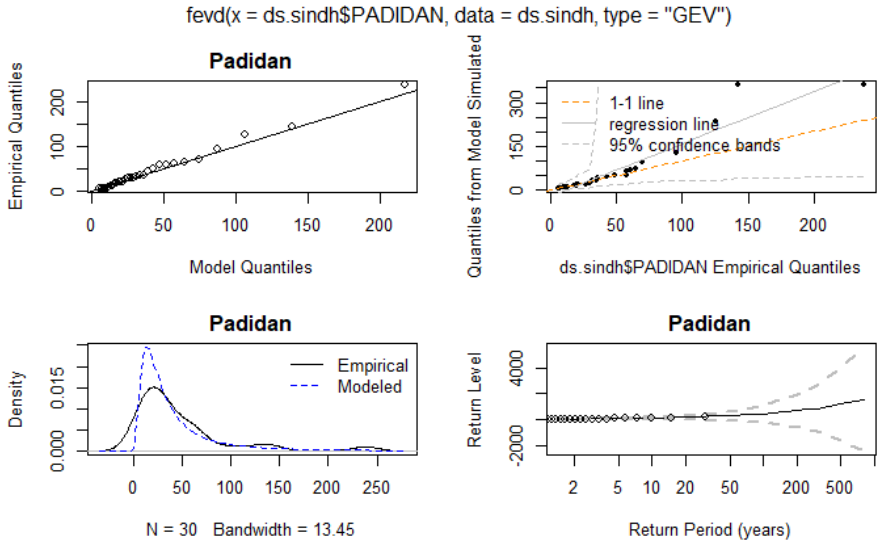

Figure D.0.26: Model Plot for the station at Padidan, Sindh

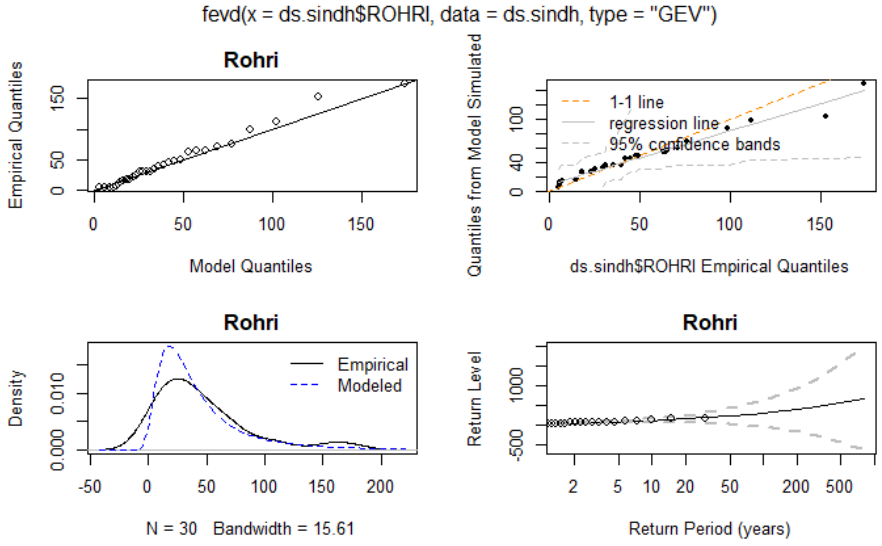

Figure D.0.27: Model Plot for the station at Rohri, Sindh

References

Anjum Bari Farooqi, Azmat Hayat Khan, and Hazrat Mir. Climate change perspective in Pakistan. *Pakistan Journal of Meteorology*, 2(3), 2005.

Mahmud M Smadi and Ahmed Zghoul. A sudden change in rainfall characteristics in Amman, Jordan during the mid 1950s. *American Journal of Environmental Sciences*, 2(3):84–91, 2006.

Anthony M Fowler, G Boswijk, J Gergis, and Andrew Lorrey. Enso history recorded in agathis australis (kauri) tree rings. part a: kauri's potential as an enso proxy. *International Journal of Climatology: A Journal of the Royal Meteorological Society*, 28(1):1–20, 2008.

PP Nikhil Raj and PA Azeez. Trend analysis of rainfall in bharathapuzha river basin, Kerala, India. *International Journal of Climatology*, 32(4):533–539, 2012.

Michele Brunetti, Michele Colacino, Maurizio Maugeri, and Teresa Nanni. Trends in the daily intensity of precipitation in Italy from 1951 to 1996. *International Journal of Climatology*, 21(3):299–316, 2001.

Ewa B Łupikasza, Stephanie Hänsel, and Jörg Matschullat. Regional and seasonal variability of extreme precipitation trends in southern Poland and central-eastern Germany 1951–2006. *International Journal of Climatology*, 31 (15):2249–2271, 2011.

Sunyurp Park. Integration of satellite-measured LST data into cokriging for temperature estimation on tropical and temperate islands. *International Journal of Climatology*, 31(11):1653–1664, 2011.

Agne Burauskaite-Harju, Anders Grimvall, and Claudia von Brömssen. A test for network-wide trends in rainfall extremes. *International Journal of Climatology*, 32(1):86–94, 2012.

Hiroyuki Iwasaki. Recent positive trend in heavy rainfall in eastern Japan and its relation with variations in atmospheric moisture. *International Journal of Climatology*, 32(3):364–374, 2012.

Robert R Gillies, Shih-Yu Wang, and Wan-Ru Huang. Observational and supportive modelling analyses of winter precipitation change in China over the last half century. *International Journal of Climatology*, 32(5):747–758, 2012.

Jianping Li, Juan Feng, and Yun Li. A possible cause of decreasing summer rainfall in northeast Australia. *International Journal of Climatology*, 32(7): 995–1005, 2012.

PT Nastos and CS Zerefos. Decadal changes in extreme daily precipitation in Greece. *Advances in Geosciences*, 16:55–62, 2008.

TP Burt and EJS Ferranti. Changing patterns of heavy rainfall in upland areas: a case study from northern England. *International Journal of Climatology*, 32(4):518–532, 2012.

NR Deshpande, A Kulkarni, and K Krishna Kumar. Characteristic features of hourly rainfall in India. *International Journal of Climatology*, 32(11):1730–1744, 2012.

Muhammad Aleem-ul Hassan, Sajjad Haider, and Kalim Ullah. Diagnostic study of heavy downpour in the central part of Pakistan. *Pakistan Journal of Meteorology*, 7(13):53–61, 2010.

Tayeb Raziei, Abbas Mofidi, João A Santos, and Isabella Bordi. Spatial patterns and regimes of daily precipitation in Iran in relation to large-scale atmospheric circulation. *International Journal of Climatology*, 32(8):1226–1237, 2012.

Stacey Dravitzki and James McGregor. Extreme precipitation of the waikato region, New Zealand. *International Journal of Climatology*, 31(12):1803–1812, 2011.

Gustavo Naumann, María Paula Llano, and Walter Mario Vargas. Climatology of the annual maximum daily precipitation in the la plata basin. *International Journal of Climatology*, 32(2):247–260, 2012.

Jürg Schmidli and Christoph Frei. Trends of heavy precipitation and wet and dry spells in Switzerland during the 20th century. *International Journal of Climatology: A Journal of the Royal Meteorological Society*, 25(6):753–771, 2005.

Olga Zolina, Clemens Simmer, Alice Kapala, Susanne Bachner, Sergey Gulev, and Hermann Maechel. Seasonally dependent changes of precipitation extremes over Germany since 1950 from a very dense observational network. *Journal of Geophysical Research: Atmospheres*, 113(D6), 2008.

Ewa Lupikasza. Spatial and temporal variability of extreme precipitation in Poland in the period 1951–2006. *International Journal of Climatology: A Journal of the Royal Meteorological Society*, 30(7):991–1007, 2010.

Christoph Frei and Christoph Schär. Detection probability of trends in rare events: Theory and application to heavy precipitation in the alpine region. *Journal of Climate*, 14(7):1568–1584, 2001.

Cecilia Svensson and Dörte Jakob. Diurnal and seasonal characteristics of precipitation at an upland site in Scotland. *International Journal of Climatology: A Journal of the Royal Meteorological Society*, 22(5):587–598, 2002.

Kenneth E Kunkel. North American trends in extreme precipitation. *Natural Hazards*, 29(2):291–305, 2003.

Muhammad Afzal and Qamar ul Zaman. Case study: Heavy rainfall event over Lai Nullah catchment area. *Pakistan Journal of Meteorology*, 6(12), 2010.

Abdul Aziz and Shigenobu Tanaka. Regional parameterization and applicability of integrated flood analysis system (ifas) for flood forecasting of upper-middle indus river. *Pakistan Journal of Meteorology*, 8:21–38, 2011.

Mian Sabir Hussain and Seungho Lee. The regional and the seasonal variability of extreme precipitation trends in Pakistan. *Asia-Pacific Journal of Atmospheric Sciences*, 49(4):421–441, 2013.

Gaston Samba and Dominique Nganga. Rainfall variability in Congo-Brazzaville: 1932–2007. *International Journal of Climatology*, 32(6):854–873, 2012.

World Commission on Dams. *Dams and Development: A New Framework for Decision-making: The Report of the World Commission on Dams*. Earthscan, 2000.

Qamar Uz Zaman Chaudhry. *Climate change profile of Pakistan*. Asian Development Bank, 2017.

Yasuaki Hijioka, Erda Lin, Joy Jacqueline Pereira, RT Corlett, X Cui, GE Insarov, RD Lasco, E Lindgren, and A Surjan. Asia. climate change 2014: Impacts, adaptation, and vulnerability. part b: Regional aspects. contribution of working group ii to the fifth assessment report of the intergovernmental panel on climate change. *Cambridge University Press, Cambridge, United Kingdom and New York*, pages 1327–1370, 2014.

M Munir Sheikh, N Manzoor, M Adnan, J Ashraf, and AM Khan. Climate profile and past climate changes in Pakistan. *Global Change Impact Studies Center (GCISC)-RR-01*, 2009.

W Iqbal, M Zahid, et al. Historical and future trends of summer mean air temperature over South Asia. *Pakistan Journal of Meteorology Vol*, 10(20), 2014.

Q-u-Z Chaudhry, A Mahmood, G Rasul, and M Afzaal. Climate change indicators of Pakistan. *Pakistan Meterological Department*, 2009.

R Rajbhandari, AB Shrestha, A Kulkarni, SK Patwardhan, and SR Bajracharya. Projected changes in climate over the indus river basin using a high resolution regional climate model (precis). *Climate Dynamics*, 44(1): 339–357, 2015.

Mian Sabir Hussain and Seung-Ho Lee. A classification of rainfall regions in Pakistan. *Journal of the Korean Geographical Society*, 44(5):605–623, 2009.

A Waqas and H Athar. Spatiotemporal variability in daily observed precipitation and its relationship with snow cover of Hindukush, Karakoram and Himalaya region in northern Pakistan. *Atmospheric Research*, 228:196–205, 2019.

Waheed Ullah, Guojie Wang, Gohar Ali, Daniel Fiifi Tawia Hagan, Asher Samuel Bhatti, and Dan Lou. Comparing multiple precipitation products against in-situ observations over different climate regions of Pakistan. *Remote Sensing*, 11(6):628, 2019.

Safi Ullah, Qinglong You, Waheed Ullah, and Amjad Ali. Observed changes in precipitation in China-Pakistan economic corridor during 1980–2016. *Atmospheric Research*, 210:1–14, 2018.

Farhat Abbas, Iqra Rehman, Muhammad Adrees, Muhammad Ibrahim, Farhan Saleem, Shafaqat Ali, Muhammad Rizwan, and Muhammad Raza Salik. Prevailing trends of climatic extremes across indus-delta of Sindh-Pakistan. *Theoretical and Applied Climatology*, 131(3):1101–1117, 2018.

Asher Samuel Bhatti, Guojie Wang, Waheed Ullah, Safi Ullah, Daniel Fiifi Tawia Hagan, Isaac Kwesi Nooni, Dan Lou, and Irfan Ullah. Trend in extreme precipitation indices based on long term in situ precipitation records over Pakistan. *Water*, 12(3):797, 2020.

Yun-Jian Zhan, Guo-Yu Ren, Arun Bhaka Shrestha, Rupak Rajbhandari, Yu-Yu Ren, Jayanarayanan Sanjay, Yan Xu, Xiu-Bao Sun, Qing-Long You, and Shu Wang. Changes in extreme precipitation events over the Hindu Kush Himalayan region during 1961–2012. *Advances in Climate Change Research*, 8(3):166–175, 2017.

Hua Xie, Claudia Ringler, Tingju Zhu, and Ahmad Waqas. Droughts in Pakistan: a spatiotemporal variability analysis using the standardized precipitation index. *Water international*, 38(5):620–631, 2013.

Muhammad Sohail Gadiwala and Farkhunda Burke. Climate change and precipitation in Pakistan-a meteorological prospect. *International Journal of Economic and Environmental Geology*, pages 10–15, 2019.

Muhammad Waseem Ashiq, Chuanyan Zhao, Jian Ni, and Muhammad Akhtar. Gis-based high-resolution spatial interpolation of precipitation in mountain–plain areas of upper Pakistan for regional climate change impact studies. *Theoretical and Applied Climatology*, 99(3):239–253, 2010.

Amir Nawaz Khan et al. Analysis of flood causes and associated socio-economic damages in the Hindukush region. *Natural hazards*, 59(3):1239, 2011.

Qing-Long You, Guo-Yu Ren, Yu-Qing Zhang, Yu-Yu Ren, Xiu-Bao Sun, Yun-Jian Zhan, Arun Bhakta Shrestha, and Raghavan Krishnan. An overview of studies of observed climate change in the Hindu Kush Himalayan (HKH) region. *Advances in Climate Change Research*, 8(3):141–147, 2017.

Muhammad Farooq Iqbal and H Athar. Variability, trends, and teleconnections of observed precipitation over Pakistan. *Theoretical and Applied Climatology*, 134(1):613–632, 2018.

Kamal Ahmed, Shamsuddin Shahid, Xiaojun Wang, Nadeem Nawaz, and Najeebullah Khan. Spatiotemporal changes in aridity of Pakistan during 1901–2016. *Hydrology and Earth System Sciences*, 23(7):3081–3096, 2019.

Syed Ahmad Hassan and M Rashid Kamal Ansari. Hydro-climatic aspects of Indus River flow propagation. *Arabian Journal of Geosciences*, 8(12):10977–10982, 2015.

Thomas J Galarneau, Thomas M Hamill, Randall M Dole, and Judith Perlwitz. A multiscale analysis of the extreme weather events over western Russia and northern Pakistan during july 2010. *Monthly Weather Review*, 140(5):1639–1664, 2012.

KL Rasmussen, AJ Hill, VE Toma, MD Zuluaga, PJ Webster, and RA Houze Jr. Multiscale analysis of three consecutive years of anomalous flooding in Pakistan. *Quarterly Journal of the Royal Meteorological Society*, 141(689):1259–1276, 2015.

Thomas F Stocker, Dahe Qin, G-K Plattner, Lisa V Alexander, Simon K Allen, Nathaniel L Bindoff, F-M Bréon, John A Church, Ulrich Cubasch, Seita Emori, et al. Technical summary. In *Climate change 2013: the physical science basis. Contribution of Working Group I to the Fifth Assessment Report of the Intergovernmental Panel on Climate Change*, pages 33–115. Cambridge University Press, 2013.

Rashid Mahmood and Shaofeng Jia. Assessment of impacts of climate change on the water resources of the transboundary Jhelum river basin of Pakistan and India. *Water*, 8(6):246, 2016.

Chad Shouquan Cheng, Heather Auld, Qian Li, and Guilong Li. Possible impacts of climate change on extreme weather events at local scale in south–central Canada. *Climatic Change*, 112(3):963–979, 2012.

Kevin E Trenberth and John T Fasullo. Climate extremes and climate change: The Russian heat wave and other climate extremes of 2010. *Journal of Geophysical Research: Atmospheres*, 117(D17), 2012.

Sajjad Haider and Shahzada Adnan. Classification and assessment of aridity over Pakistan provinces (1960-2009). *International Journal of Environment*, 3(4):24–35, 2014.

AP Dimri, D Niyogi, AP Barros, J Ridley, UC Mohanty, T Yasunari, and DR Sikka. Western disturbances: a review. *Reviews of Geophysics*, 53(2): 225–246, 2015.

SARDAR Sarfaraz, MUDASAR HASAN Arsalan, and HIRA Fatima. Regionalizing the climate of Pakistan using köppen classification system. *Pakistan Geographical Review*, 69:111–132, 2014.

Danuta Martyn. Climates of the world. *Developments in Atmospheric Science*, 18, 1992.

Steven K Walterscheid. *Climate classification for the earth's oceanic areas using the KOppen System*. PhD thesis, Kansas State University, 2011.

K Nasrullah. Climate of west Pakistan according to thornthwaite system of classification of climates, pgr vol. 23 (no. 1): 12-25. *Pakistan Geographical Review*, 17(1):1, 1962.

RA Houze, KL Rasmussen, S Medina, SR Brodzik, and U Romatschke. Anomalous atmospheric events leading to the summer 2010 floods in Pakistan. *Bulletin of the American Meteorological Society*, 92(3):291–298, 2011.

Kieran MR Hunt, Andrew G Turner, and Len C Shaffrey. Extreme daily rainfall in Pakistan and north India: Scale interactions, mechanisms, and precursors. *Monthly Weather Review*, 146(4):1005–1022, 2018.

AP Dimri. Surface and upper air fields during extreme winter precipitation over the western Himalayas. *Pure and Applied Geophysics*, 163(8):1679–1698, 2006.

John V Hurley and William R Boos. A global climatology of monsoon low-pressure systems. *Quarterly Journal of the Royal Meteorological Society*, 141 (689):1049–1064, 2015.

D Panagoulia, P Economou, and C Caroni. Stationary and nonstationary generalized extreme value modelling of extreme precipitation over a mountainous area under climate change. *Environmetrics*, 25(1):29–43, 2014.

Richard Von Mises. The distribution of the largest of n values. *Rev. math. Interbalkan Union*, 1:141–160, 1936.

Arthur F Jenkinson. The frequency distribution of the annual maximum (or minimum) values of meteorological elements. *Quarterly Journal of the Royal Meteorological Society*, 81(348):158–171, 1955.

Stuart Coles. Classical extreme value theory and models. In *An Introduction to Statistical Modeling of Extreme values*, pages 45–73. Springer, 2001.

Jan Beirlant, Yuri Goegebeur, Johan Segers, and Jozef L Teugels. *Statistics of Extremes: Theory and Applications*, volume 558. John Wiley & Sons, 2004.

Henry B Mann. Nonparametric tests against trend. *Econometrica*, pages 245–259, 1945.